2009-08-11

Microanalysis of Heterogeneous Radiation in Particulate Matter as an Aid to Nuclear Source Identification

Marco Paul Johann Kaltofen
Worcester Polytechnic Institute

Microanalysis of Heterogeneous Radiation in Particulate Matter as an Aid to Nuclear Source Identification

by

Marco Kaltofen

A Thesis

Submitted to the Faculty

of the

WORCESTER POLYTECHNIC INSTITUTE

In partial fulfillment of the requirements for the

Degree of Master of Science

in

Environmental Engineering

By

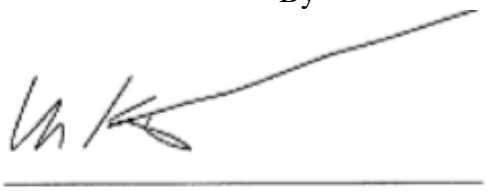

Marco Kaltofen, PE, (Civil, Mass.)
August 4, 2009

Approved by: 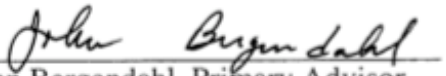
John Bergendahl, Primary Advisor

Approved by: 
Tahar El-Korchi, Dept. Head

ii - ACKNOWLEDGEMENTS

I would like to thank my advisor, John Bergendahl, at the Department of Civil and Environmental Engineering for his encouragement, advise and direction, and most especially for his patience in helping a lifelong field engineer learn how to approach the very different world of research.

I would also like to thank Don Pelligrino for assistance with atomic spectrometry, and for making students such as myself feel welcome in the laboratories. Shawn Strong Bear, of Boston Chemical Data Corp., provided important autoradiography assistance. I received instrumentation support from Rafeal Garcia, at the Department of Physics, and also from WPI senior undergraduates Mathew Silva, Joseph Mullen, and Dericc Orso, who worked under the direction of Prof. Garcia.

I would like to gratefully thank Dr. Rudi H. Nussbaum of Portland State University for funding the commercial gamma and alpha spectroscopy required for this project, and for providing information on radioactive iodine isotopes. Dr. Nussbaum is a contributor to the Center for Disease Control's Toxicological Profiles for ionizing radiation, cesium, iodine-131, plutonium, and radon.

Split sampling and analysis of some environmental samples collected for this study was performed through the offices of the Los Alamos National Laboratory and the State of Washington Department of Environment.

Assistance with travel expenses came from a supporting grant from the Ploughshares Foundation and the Oregon Community Foundation, administered by Hanford Challenge, a public interest 501.c3 corporation, whose url is, www.hanfordchallenge.org. The staff of this private organization, dedicated to public health, environmental safety, and economic stability, seems as much a partner at Hanford as is the Department of Energy. I am privileged to be on HC's Board of Directors.

Sampling support was provided by Tom Carpenter and Hanford Challenge, the Government Accountability Project, Peter Takeda, author of Eye at the Top of the World, Sergei Pashenko of Siberian Scientists for Social Responsibility, German Lukashin of the All Russia Scientific and Research Institute of Technical Physics, the Yakama Indian Nation of Wapato, WA, the San Il Defenso Indian Nation of San Il Defenso Pueblo, NM, Tim Connor, and the Spokane Indian Nation of Wellpinit, WA. I am particularly grateful to the many First Nation people and their own officials, who welcomed me and this project, and made it possible to sample in their homes and on their lands.

Thank you to my daughter Beryl for accompanying me to Richland, WA while I collected dust samples, and for crashing gracefully at the home lent to us by two Sandia Labs nuclear engineers; and to my youngest daughter Savannah, who played with dolls at Los Alamos while I prattled on about hot particles with local residents, First Nation Governors, and New Mexican officials. I hope it was educational for you both. It was a grace for me.

I am very grateful to my wife, Christine Schell, for her patience when the tapping of laptop keys became the background music of our evenings, and for her encouragement, even as I embarked on my many sample collection trips. When a married person gets a graduate degree, there should be room for two names on the diploma.

Table of Contents

Appendix A: Sample locations, descriptions, and field notes

Appendix B: On DVD-ROM, gamma spectrometry data

Appendix C: On DVD-ROM, SEM/EDS data

Appendix D: On DVD-ROM, PACE gamma spectrometry data

iv - List of Figures

v - List of Tables

vi – HYPOTHESIS

The origin of radionuclide contamination in environmental samples can be determined by microanalyses of individual hot particles. Microanalysis can be more sensitive than the gross analyses of bulk samples. Radioactive heterogeneity in a sample of particulate matter can be quantified with a simple mathematical expression.

vii – ABSTRACT

Radionuclides in particulate matter associated with outdoor and indoor dusts were analyzed to determine the form and concentration of radioactive isotopes present. These radioactive isotopes, such as Strontium 90, Cesium 137, and Uranium 235, consist of, or are sorbed onto fine particulate matter, (PM). The airborne dispersion of this fine particulate matter results in the facilitated transport of these sorbed or neat radionuclides. Sources of particulate-bound radioactive contaminants include fallout from weapons testing, accumulation of radon daughters, transport of soils containing naturally-occurring radioactive material, remediation of radiologically-contaminated sites, and nuclear material processing. Radiological contaminants in PM, may exist as trace contamination in homogenous collections of particles, but may also exist heterogeneously, as a small number of high-concentration radionuclides among a larger set of uncontaminated particles. A total of 114 samples of indoor and outdoor airborne dusts were collected from a former nuclear weapons production facility near Richland, WA, the Los Alamos National Laboratory, and the Yakama Indian Nation in Wapato, WA.

Los Alamos, NM was also the site of the May 2000 Cerro Grande wildfire. The wildfire created very large amounts of airborne particulate matter, including smoke and soot. The area affected by open burning included 43,000 acres. At the national laboratory, greater than 7600 acres were affected, including some areas that were radiologically-contaminated, such as a U-238 ammunition firing area. (LANL, 2007) This introduces a potential source of hot particles in dusts and other archived particulate matter, which may

remain in the environment. LANL Airborne radionuclide surveillance has historically found higher uranium levels during windy periods, and saw elevated air uranium levels associated with the Cerro Grande fire. (Ibid, p. 108)

Dust samples were sieved to pass a 150 micron screen and analyzed by gamma spectroscopy. Samples with higher activity were analyzed by Scanning Electron Microscopy/Energy Dispersive X-ray analysis, SEM/EDS. The results of gamma spectroscopy and individual particle counts were compared to determine the degree of radioactive heterogeneity in each sample. Radioactive heterogeneity, isotopic distribution, and particle size can be related to the source of the radioactive PM.

Radiological contaminants in particulate matter, (PM), may exist as trace contamination in homogenous collections of particles, but may also exist heterogeneously, as a small number of high-concentration radionuclides among a larger set of uncontaminated particles.

Residential and source area dusts were collected from locations surrounding, and potentially impacted, by operational and remedial activities at the HNR. The dust samples were analyzed, by multiple means, in order to identify those with radiologically-contaminated particles. Samples with higher activity were further analyzed by Scanning Electron Microscopy/Energy Dispersive X-ray analysis, (SEM/EDS), to determine if the radiological contamination was homogenous or heterogeneous.

Two case studies were followed. The method isolated and analyzed lead and bismuth from naturally occurring radioactive material in coal fly ash. The method isolated and fingerprinted thorium, and the rare earths cerium, lanthanum, samarium, neodymium, and gadolinium in sedimentary cerium monazite minerals, nuclear waste processing dusts, and fission waste products in a WWTP effluent channel.

Chapter 1 - What problem motivated this research?

The existence of hot particles, particles containing substantially more radioactive material than surrounding matter, has been of interest in studies of radioactivity in environmental and industrial settings. Hot particle environments are found in nuclear power plants, and in nuclear fuel fabrication and reprocessing facilities. (Sajo-Bohus, 1998) It has been postulated that hot particles lead to health impacts different from exposure to equivalent amounts of uniformly-distributed radiation delivered without hot particles. (Lang, 1995) Hot particles have been detected in the environment, at significant distances from presumed source sites. (Broda, 1987)

Nuclear weapons testing generates spherical hot particles in the 10 micron to submicron size range. Testing generates particles which exceed 100 microns in size, where "larger particles are more apt to consist of fission products condensed on dust convected from the ground." (Eisenbud, 1953) Airborne particulate testing performed during the period of active atmospheric nuclear weapons testing found no correlation between weight or number of particles collected and total activity. (Shleien, 1965) This result is consistent with hot particle capture. Radon gas generates daughter products which condense into nanometer-sized particles. Indoor radon progeny particulates, from stoves and heaters, are in the 20 to 80 nm size range, while those from cigarette smoking and frying are in the 100 to 200 nm range. (George, 1991)

The presence of gross sample activity, or of activity related to a single radionuclide such as Uranium 238 or Strontium 90, does not give sufficient information to determine the source of the detected radioactivity. Additional analyses are required to determine if the origins of any radiologically-contaminated particulate material, (PM), can be assigned to specific sources.

Samples can be characterized based upon original location, particle size distribution, morphology, mineral components, gross alpha, beta, and gamma radiation, and the concentrations of individual radionuclides. Location data includes both geospatial data

and the immediate location of dust accumulations within residences such as those from attics, carpets, or appliances. Morphology considerations center around artifacts of pyrolytic processing, and on the relationships between particle size, settling velocities, and long-range transport potential.

Samples can also be characterized based upon whether their activity is uniformly distributed, or heterogeneous. In a uniformly distributed sample, total radioactivity is function of mass or surface area of PM.

In a heterogeneously distributed sample, total activity is a function of the summed activity of each individual particle, and not fully dependent on the total mass or surface area of PM. Heterogeneity in the distribution of radioactive material in a sample occurs when a subset of particles in a sample contain higher levels of radioactivity than the remaining particles in a sample. In the maximally heterogeneous sample, 1 particle would account for 100 % of the total activity, and the remainder would be inert.

This heterogeneity can exist at more than one level. Consider three possible types of hot particles. Hot particles can form from processing or erosion of bulk radioactive materials, such as the formation of uranium dusts from uranium ore milling or enrichment. Hot particles can exist as condensates from gases, (ref. Friedlander, S., 2000), such as solid particles, or aggregates of particles, formed by the radioactive decay of radon gas. Gaseous materials, such as radioiodine, may be adsorbed to the surface of clay particles. (Adsorption – "the net accumulation of a chemical species at the interface between a solid phase and an aqueous solution phase" from Sposito 1989, or in this case, at the interface of a solid and a gas)

Iodine-131, a radioactive gas, can sorb onto PM. (Nussbaum, 2008) Radioactive iodine is released during the chemical separations processing of irradiated uranium fuel assemblies. Dissolution of the assemblies in nitric acid releases airborne effluents. Along with I-131 and I-129, this process also releases Ce-144, and Ru-103 and Ru-106. (Hanford CHRP, 2002) I-129 is a gas which is known to sorb to PM. I-131 also behaves

in the same manner, but its halflife is too short to be useful in this study. The halflife of I-131 is 8.0 days. (ATSDR 2002) Any I-131 sorbed onto sampled PM has decayed below detectable limits, as some dust accumulations may be months or years old at the time of sampling. (Cizdziel, J. V., Hodge, V. F., 2000),

In the last of the three examples, the hot particles themselves are heterogeneous, with varying specific activity across different portions of particle. This heterogeneous distribution is the result of the process which formed the particle. Thus the distribution itself gives information about how the hot particle was formed. (ref. R. Nussbaum, 2008)

1.2 Environmental Implications

Analyzing an individual particle overcomes the diluting effects of particle dispersion in the environment. Individual particle analyses have greater sensitivity because no signal or noise is acquired from inert material, as happens with bulk sample analyses. The added information gained from a clear view of a discrete particle can assist in determining the origin of radiation at an environmental location.

This report focuses on specific questions about the source of radioactivity in environmental media. The first involves the occurrence of thorium and rare earth elements in environmental materials. This combination can be the result of both natural and industrial nuclear processes. This type of hot particle was found in river sediments, and in dusts collected from Hanford workers' clothing. Hot dust particles lost from nuclear reactors or nuclear materials processing are colloquially referred to as fission fleas. These "fleas", once trapped and analyzed, provide important information about the processes which created them.

In both media, the morphology and chemical/radiological constituents of the particles were strikingly similar. The particle sizes were quite different, as would be expected from airborne vs. waterborne particles, where water can generally suspend larger

particles than ambient air. The appearance of nearly identical thorium rare earth particles in two environmental media, sediment and workplace dusts, suggests a more complex origin for these monazites than could be explained by river sediment transport alone. This insight would not be apparent from gross analyses alone, as the thorium and rare earths signal would have been hard to distinguish from the overall noise.

For the Thorium - rare earth example, four sampling sites visited for this study displayed near-background level radiation related to thorium and uranium. (Thorium is part of the uranium decay series.) Gross analyses did not yield sufficient information to discriminate between potential sources of these low level alpha emissions. Neither did gross analyses provide sufficient information to determine the chemical nature of source material which caused the low level gamma emissions at energy lines associated with uranium and thorium. These emissions could have come from fission products, or from naturally-occurring radioactive materials, (NORM). Signal to noise ratios were too low to detect radionuclides other than thorium and uranium-related materials.

By definition, hot particles contain greater than background concentrations of radionuclides. Gross background concentrations are highly location-specific. No single value is the background level for large regions. Nevertheless, one of the key features of this investigation has been the collection of useful environmental radiological information from samples whose gross radioactivities are close to background.

Concentrations of a radioisotope in excess of background levels, do not, by themselves, necessarily indicate an anthropogenic source of radiation. For example, the thermal features in the Yellowstone, Wyoming Caldera can concentrate cesium from 7.6 ppm in unaltered rock to 3000 ppm in altered sediments. (Terry, 1983, abstract) The same caldera features also concentrate uranium via dissolution/precipitation in groundwater. (Sturchio, 1987, abstract)

The following notes on background radiation are specific to the Hanford and Los Alamos sites, and were written for the Pacific Northwest National Laboratory. (Patton, 2005)

These, (edited), data give a short review of both impacted and unimpacted site levels of various radionuclides.

> "Naturally-occurring potassium-40 was present at levels above detection in all sediment samples taken by each agency." (range: 18.7 pCi/g to 8.2 pCi/g)
>
> "Uranium was measured in all sediment samples at levels above detection" (range: 3.56 pCi/g to 0.9 pCi/g) The concentrations of uranium in soils adjacent to the Hanford Fuel Fabrication Facility near Richland, Washington ranged from 0.51 to 3.1 pCi/g."
>
> "Plutonium-238 concentrations were below DOH's low limit of detection (0.03 pCi/g) for all samples. The highest concentration of plutonium-239/240 was 0.049 pCi/g.
>
> "Cesium-137 ranged from 0.094 to 0.63 pCi/g."
>
> "Strontium-90 - The background samples analyzed by PNNL from Priest Rapids contained 0.00326 and 0.0104, [nondetects]"

Upon isolating hot particles, and analyzing these via SEM/EDS, the sizes, morphologies, and compositions of the particles were detailed. Upon inspection, it was evident that the Calcium phosphorous minerals, specifically cerium monazites, were present in many of our samples. One sample, postulated to be contaminated with either NORM or fission products, contained particles consisting of thorium, uranium, and rare earth elements, but without detectable calcium or phosphorous.

Thorium monazites are an environmentally significant source of thorium, and long known as an alternate source of fissionable material for civilian power reactors. (Science, 1939) Neutron bombardment of thorium 232 creates fissionable U233 as a decay product. (ref. Argonne NL 2005, See also Chapter 5 – Environmental significance of results)

1.3 Health Effects of Fine Particulate Matter and Hot Particles

Hot particles result in human health effects caused by inhalation of particulate matter generally, and also due to the radioactive nature of these respirable particulates. The US Environmental Protection Agency web-based information sheet on common air pollutants, (www.epa.gov/particles/health.html), notes that,

> "Particle pollution - especially fine particles - contains microscopic solids or liquid droplets that are so small that they can get deep into the lungs and cause serious health problems. Numerous scientific studies have linked particle pollution exposure to a variety of problems, including: increased respiratory symptoms, such as irritation of the airways, coughing, or difficulty breathing, for example; decreased lung function; aggravated asthma; development of chronic bronchitis; irregular heartbeat; nonfatal heart attacks; and premature death in people with heart or lung disease."

This same US Environmental Protection Agency source notes further that,

> "The size of particles is directly linked to their potential for causing health problems. Small particles less than 10 micrometers in diameter pose the greatest problems, because they can get deep into your lungs, and some may even get into your bloodstream."

Exposure to such particles can affect both your lungs and your heart. Small particles of concern include "coarse particles" (such as those found near roadways and dusty industries), which are larger than 2.5 micrometers and smaller than 10 micrometers in diameter; and "fine particles" (such as those found in smoke and haze), which are 2.5 micrometers in diameter and smaller. To these general effects of exposure to particulates, one adds the further health burden of exposure to ionizing radiation from the hot particles. Fine hot particulates are trapped by lung and bronchial tissues, where the cells surrounding the particle may experience sufficient radiation exposure to cause cell death. Cells at greater distances may not experience sufficient energies to cause cell death, but may survive with damaged DNA or DNA repair mechanisms, resulting in

uncontrolled cell growth and reproduction, that is, tumor formation. If the particle is coarse enough to be intercepted by normal particle removal mechanisms, then the radiation exposure becomes, not a circular area of damage, but a much larger track of exposure, as the particle is expelled from the body. Natural lung clearance mechanisms thus result in a much greater number of cells exposed to radiation. (Lang, 1995)

1.4 Particle Size and Particle Properties

Transport of, and adsorption to particles are both related to the size distribution of the particles. Adsorption is, "the net accumulation of a chemical species at the interface between a solid phase and an aqueous solution phase." (From Sposito, G., 1989) In this study, the interface is likely to be between a solid and a gas.

As the average particle size decreases in a sample, the total surface area and specific adsorbtion increase. The capacity of a given mass of particles to adsorb chemical species increases with increasing surface area. The relationship between surface area and capacity to adsorb chemical species is described by G. Sposito, and in the definition of specific adsorption, "Ions become specifically adsorbed when short-range interactions between them and the *interphase* becomes important. They are believed then to penetrate into the inner layer and may (but not necessarily) come into contact with the surface. They are usually assumed to form a partial or complete monolayer." (refs. IUPAC Compendium of Chemical Terminology 2nd Edition, 1997; Spositio, 2008, Ersahin, 2006)

An example of the relationship between decreasing particle size and increasing chemical species concentration is seen in Friedlander, S. K., 2000, *Smoke, Dust, and Haze, Fundamentals of Aerosol Dynamics*, p.23, citing Davison, 1974. In this example elements in coal fly ash particles show pronounced concentration trends with respect to particle size. Concentrations of trace metals increase by a factor of 1.5 to 4.4 times as particle sizes decrease from > 11.3 microns to 1.1 to 2.1 microns. While this relationship is not universal, this analysis of coal fly ash is one example of how particles of varying

size experience varying chemical separations environments.

Particle size and density have affects on transport properties via the relationship of these variables to settling velocity. In one study, (ref. Friedlander, 2000, p. 34), as particle diameter dropped from 100 to 20 microns, for a given, fixed, set of conditions, settling velocity dropped from 30 cm/s to 1.2 cm/s. Above 100 microns, airborne particle transport becomes less significant, given the high settling velocities of larger particles. Likewise, denser particles, with higher mass to diameter ratios, have higher settling velocities. (Ibid)

Summarizing, smaller-sized particles better facilitate the transport of adsorbed species, including radioactive species, through enhanced adsorption to a given mass of particles, and reduced particle settling velocities in air, which encourages aerosol formation.

1.5 Summary of Methods and Particle Characteristics

The steps involved in detecting and isolating hot particles include:

- Field screening of environmental samples of dusts, sediments, and soils
- Gamma spectrometry screening for total radiation and radionuclide ID
- Separation of hot particle-enriched fractions, sieving, autoradiography
- SEM/EDS analysis of selected samples
- Mathematical treatment – determination of degree of heterogeneity
- Review of Environmental variables affecting particle transport

Knowledge of environmental transport phenomena assists in selecting samples for analysis. These intentional biases increase the number of hot particles collected per sample. Representative sampling would reflect different sampling objectives compared to this study, such as using representative sampling to determine the true concentration of hot particles in environmental media. An example of this environmental bias is the

collection of dust samples from hot zone workers' clothing at the Hanford Nuclear Reservation, rather than from, (for example), high volume air samples well outside the Reservation perimeter.

In this study, hot particles were typically absent from randomly selected environmental materials, particularly if there were no known area sources of anthropogenic hot particles. An exception to this generalization are particles that result from radon and uranium decay. These naturally-occurring materials are commonly found in the environment. Radon and bismuth, and bismuth/lead particles, (radon decay products), were among the most common hot particles detected, in environmental samples and in materials such as coal fly ash.

Biased sampling, based on hypothesized environmental transport vectors from presumed hot particles sources, provided large numbers of hot particles for study. (Biased sampling uses observable or predictable phenomena to guide the selection of environmental samples, ref. USEPA Reg. 4, 2005) Notably, even for randomly collected samples, "brute force methods" that collect larger numbers of particles for analysis could identify very disperse hot particles, given sufficient levels of effort, and some potential common particle source, such as uranium decay products.

The composition, particle size, morphology, mineral associations, distribution and heterogeneity, and solubility of hot particles can provide data on the potential source(s) of these particles.

Composition and Area: The composition of individual hot particles is determined analytically by SEM/EDS, along with particle size, and morphology. These data can be compared to known materials from radiogenic processes. SEM/EDS gives two dimensional data on the area of particles, which, when combined with data on compound and element densities, yields the approximate mass of individual or the mass of the total set of hot particles in a sample. This presumes that particle volumes can be estimated from particle diameters and areas.

Particle size: Household dusts are generally found in the 1 to 20 um size range, based on optical and scanning electron microscopy of 40 of the dust samples collected for this study. Literature notes that weapons detonation fallout is in the 0.5 to 2 um size range, (Eisenbud, 1953). Particles formed from the condensation of radon daughters are nanometer-sized, (McNaughton, 2008, citing George 1991, Friedlander, S., 2000), and positively charged. (Radford, 1985)

Mineral associations: Many hot particles are associated with particular minerals or industrial process materials. For example, thorium/lanthanide monazites, which may be also contain uranium oxides, will have nonradioactive accompanying elements, such as P and Ca, which are distinct markers for these minerals. Conversely, nuclear reactor fission products will contain thorium, uranium, and lanthanides, as well as Pu and Am, but may lack P and Ca. The nonradioactive elements detected by SEM/EDS can help categorize the likely source of individual hot particles.

Morphology: RPM can be distinguished by their crystalline form, fallout particles which had typically spherical form, and subangular, sorted and eroded sediment particles.

Distribution: The physical distribution of radioactive material within a bulk sample can provide data on its origin. For RPM from nuclear fission waste, heterogeneous surficial radioactive deposits were detected as evaporites on mineral substrates. Uniform radioactive coatings on clays can result from precipitation of radioactive solutes. RPM can be heterogeneous, existing as neat particles within an inert bulk material, implying a distinct origin for the RPM compared to the bulk material.

Solubility: In chemical and radiochemical analytical preparations, solubility is an important separation method, but it destroys the information on particle size, morphology, and so on, unless it only has the effect of removing soluble inerts from insoluble particles. Solubility is not examined in this research.

Location: The type of dust collected can affect results, particularly if this location change affects the time frame during which dusts accumulate. For example, attic dusts can act as archives for materials collected decades earlier, as they are relatively undisturbed. (Lioy, 2003 and Cizdziel, 2000) Dusts on surfaces may represent short term accumulations, that is, only as old as the time of the most recent surface cleaning. Appliance filter or condenser dusts, such as those found on refrigerators, are more representative of dust accumulation since the most recent cleaning. (Isosaari, 2001) In this study, refrigerator dusts accumulations varied widely, with some being relatively dust free, (cleaned recently or newly purchased/installed), and others being heavily encrusted with 1 cm or more or layered, greasy dusts.

Chapter 2 - Background

The total radiation in a homogenous sample of particles or dusts can be described by:

$$Rad = M \times \sum SA_i \quad (2.1)$$

Where M is the sample mass and SA_i is the specific activity of each radioisotope present. For a single particle in a homogenous sample, the total radiation from a sample is described by the equation:

$$Rad = M_j \times N \times \sum SA_i \quad (2.2)$$

Where M_j is the mass of the jth particle, and N is the number of particles in the sample. For a set of identical particles, the function M_j is replaced by m, the mass of each particle.

$$Rad = m \times N \times \sum SA_i \quad (2.3)$$

For a heterogeneous set of particles is a sample, the total radiation from the sample is described by the equation:

$$Rad = \sum (M_j \times \sum (SA_i \times MF_i)) \quad (2.4)$$

Where MF_i is the mass fraction of radioisotope (i) in particle (j). M_j for a specific particle is difficult to determine directly. An approximation of M_j can be found by determining the area of a specific particle microscopically. Replacing M_j with a variable based on area and density yields:

$$Rad = 4\pi/3 \sum ((area_j/\pi)^{3/2} \times \sum (SA_i \times MF_i \times density_i)) \quad (2.5)$$

A more computationally intensive version of this expression would employ a rotation of the actual two dimensional shape, (as determined by SEM), to yield a volume, rather than assuming sphericity. The function, $f(\text{area}_j)$, is the volume of the particle, as determined by computationally performing a rotation around a central axis, of the two dimensional particle shape determined by SEM. The method remains a practical rather than an exact expression, but adds an electronic computation to find the volume, yielding a more precise result.

$$\text{Activity} = \sum \left(f(\text{Area}_j) \times \sum \left(\text{SA}_i \times \text{MF}_i \times \text{density}_i \right) \right) \qquad (2.6)$$

These equations are practical for heterogeneous samples. Homogenous samples are described by the more basic expression.

$$\text{Activity} = \text{Sample Mass} \times \sum \left(\text{SA}_i \times \text{MF}_i \right) \qquad (2.7)$$

Measures of sample homogeneity

Developing a simple statistic for describing radiographic sample heterogeneity may assist in describing sample results. A simple term for describing heterogeneity is a useful way to describe environmental dust samples, because these often contain a complex mixture of materials. Some possible expressions for radiographic sample heterogeneity follow.

The uniformity coefficient is a measure of variation in particle sizes. The coefficient is defined as the ratio of the sieve size that will permit passage of 60% of particles in a sample by weight to the sieve size that will permit passage of 10% of particles in a sample by weight. Uniformity coefficients are equal to or greater than 1, with the coefficient rising as sample heterogeneity rises.

An analog to the uniformity coefficient for specific activity in particles would be the ratio of the 60th percentile activity, (on a specific, per particle basis), of a sample set to the

activity of the 10th percentile of the sample set. This is an inconvenient measure as it could require knowledge of the specific activities of all particles in a sample or population of particles. An approximation of this measure would require reviewing only the number of particles which account for 90 % of total activity, rather than 100%. This is practical for relatively heterogeneous samples, but impractical for homogenous ones.

An alternative measure of sample heterogeneity for environmental samples would be the sample standard deviation of the specific activity of a set of particles, where the population mean is defined as the specific activity of the particle population measured, (which already incorporates a denominator, mass), and the sample size is the set of n individual particles with known specific activity within that population. By this method, one can approach the true value of sample heterogeneity as the number of individual particles counted rises.

In the terms of basic statistics, the coefficient of variation is defined as the ratio of the standard deviation to the mean of a sample set. For this case, the mean is the central value of the total activity per particle. Assuming a normal distribution, the range which is two times the standard deviation would encompass the central 68.3th percentile of the particles, as measured by the total activity per particle. This method suffers from the need to measure the activity of the entire particle set, or that of a statistically significant sample of the population of particles.

For samples with a small number, n, of hot particles, a simpler measure can suffice. For n, the number of particles responsible for at least 60 % of a sample's total activity, and N, the total number of particle in a sample, sample heterogeneity based on activity can be described as:

$$\textbf{Heterogeneity} = -\log\left(1.67 \times n / N\right) \qquad (2.8)$$

The selection of the 60^{th} percentile is based upon three criteria. This percentile is equivalent to the high percentile found in the already accepted uniformity coefficient. It

also reflects a majority of the radiation in a sample. Employing a level below the 50th percentile can result in a high heterogeneity value for a sample, where the greatest part of radioactivity is contributed by uniformly-distributed radiation. A 68.3rd percentile, representing the area encompassed within one standard deviation in a normal distribution is acceptable, but implies that hot particles would be normally distributed. Given that as few as one or two hot particles may contribute the bulk of radioactivity in a sample, the implication that heterogeneous radiation is normally distributed may be demonstrably false. For heterogeneous samples with a single hot particle, calculating standard deviation is not meaningful, and results in a divide by zero error.

For the highly heterogeneous thorium-containing silt sample collected on the Columbia River, n = 2 and N is approximately 10,000. (Based on autoradiography to determine n and optical microscopy to estimate N). The sample heterogeneity is 3.5. This function decreases below 0.001 as n approaches 0.6 times N, meaning the sample is more uniform in its distribution of specific activity. The value of n/N must be between 0.6 and 1/N.

The degree of sample heterogeneity could also affect an analysis of the source of environmental radioactivity. The presence of a high level of sample heterogeneity suggests that a separation process of some kind is occurring. Determining the nature of that separation process may give insight into the activity's source.

Consider a hypothetical example of hot particles in an unsorted sediment, which contains hot particles that have a median particle size of 100 microns, and a standard deviation of 10 microns. The size distribution of the hot particles is substantially different from the size distribution of the inert material. This difference suggests that the hot particles have a source distinct from the sediment generally. These distinct size distributions could result from the contamination of the sediment by a specific radioactive waste material. The radioactive material transport remains primarily a function of sediment transport, but the origin of the hot particles is not the same as the whole sediment. Had the hot particle size distribution been centered about a much lower value, such as 1 micron, then washout of global or local radioactive fallout would be a plausible origin as well.

If instead the sediment were uniformly radioactive, (no hot particles present), then radioactive material transport may be more likely due to the presence of radioactive material in the sediment parent material or precipitation of an initially dissolved radioactive material.

Natural weathering processes can result in the heterogeneous redistribution of naturally-occurring radioactive material, (NORM). An example for leaching and redistribution of uranium is given in Hamilton, 1966.

Particle counting

One can assume that a separation and hot particle analytical scheme could separate and identify all or most of the hot particles in a sample. In such a case, the total radiation in the sample, as measured by gross means, can be compared to the calculated, (or measured), radioactivity in the hot particles.

EXAMPLE: A 1.0 gram sample of dust is counted and found to contain 2.6 pCi of gamma radiation. Assuming a total counting efficiency of 20 %, the true specific activity of the dust sample is 13 pCi. (Counting efficiency varies with detector, sample geometry, and distance from detector to sample. At 100 keV, NaI detectors may have total counting efficiencies in the range of 15 % to 43 %, with shorter sample to detector distances giving higher total efficiencies. Ref. Yalcin, 2007)

This activity could be spread uniformly among the particles of the dust sample. Alternatively, the sample could contain a total of five Ra226 particles, each with a diameter = 1 um, that would likewise yield 13 pCi. In the first case, the sample is fully uniform, and in the second, it is fully nonuniform. The sample could also have a single

Ra226 particle, with a diameter equal to, (in microns), the cube root of 5.0, with the same result.

TABLE 2.1: Particle Dimensions, mass and specific activities, (SA = specific activity)

Length (L)	Cube Vol. S = L	Sphere Vol. D = L	Cube Mass d = 1	Sphere Mass d = 1	Sphere SA Ra226	Sphere SA Th230	Sphere Mass Th230
1 cm	1 ml	0.52 ml	1.0 g	0.52 g	2.6 Ci	0.12 Ci	6.1 g
1 mm	1 ul	0.52 ul	1.0 mg	0.52 mg	2.6 mCi	0.12 mCi	6.1 mg
100 um	1 nl	0.52 nl	1.0 ug	0.52 ug	2.6 uCi	0.12 uCi	6.1 ug
10 um	1 pl	520 um3	1.0 ng	0.52 ng	2.6 nCi	0.12 nCi	6.1 ng
1 um	1 fl	0.52 um3	1.0 pg	0.52 pg	2.6 pCi	0.12 pCi	6.1 pg

For a 1.0 gram population of uniformly-sized nonradioactive dust particles, all of diameter 1 ug, the total number of particles is 1.0 EE 12. The CERCLA soil cleanup criteria is 5.0 pCi/g of alpha emitters, (ref. 40 CFR 192). Adding two radium particles of diameter = 1.0 um to the population would exceed this criteria, at 2.6 pCi x 2 = 5.2 pCi. The sample heterogeneity is 11.5 for this, relatively extreme, example.

A Selection of Relevant Scientific Literature

Previous researchers have reviewed hot particles and their environmental significance. Individual peer-reviewed scientific journal articles have covered many of the topics in this report. Each of the publications noted below describes one of the steps in this overall procedure for isolating and analyzing hot particles, as described in this study. They provide a literature basis for the use of each of these techniques in the analytical methods used in this study. Each of these peer-reviewed articles is an early, or simply typical citation of a procedure of principle which, when synthesized, allowed hot particles to be detected, isolated, or better understood in this study.

Two things distinguish this previously published research from this study. 1 – The specific methodology for selecting environmental samples, separating hot particles, and completing their analysis required using the sequential use of the techniques described in all of these articles, together. 2 – Using these combined techniques as a coherent microanalytical method, was sufficient to find solutions to specific environmental questions on the origin of radioactivity in environmental media.

Autoradiography - A practical and proven technique for visualizing the quantity and location of particulate matter which contains radioactive material. The 1954 study by H. Clark detailed hot particles on outdoor plants related to fallout from nuclear test detonations in the Troy, New York area. This is an excellent discussion of the simplicity of autoradiography, and its use to relate the particulate form of radiation carriers to their origin. (Clark, H. M., 1954) D. McCubbin reviewed marine sands contaminated by particulate matter related to the Windscale reactor fire. (McCubbin, D., 2000)

Fallout particle morphology – Includes a description of particle size and the relationship between size and particle formation processes – One of many fallout related articles generated during the peak atmospheric testing years, culminating in the 1963 testing activity maximum - Eisenbud, M., and Harley, J., (1953), *Radioactive Dust from Nuclear Detonations*, Science, New Series, Vol. 117, No. 3033, Feb. 13, pp. 141-147

Hot particles – health implications - Lang, S., Servomaa, K., Kosma, V.-M., Rytomaa, T., (1995), *Biokinetics of Nuclear Fuel Compounds and Biological Effects of Nonuniform Radiation*, Environmental Health Perspectives, Vol. 103, No. 10. Oct., pp. 920-934. The health effects of doses received from particulate-based radiation may be distinct from effects received on a whole body basis.

Hot particles and global transport Shleien, B., et al, (1965), *Particle Size Fraction of Airborne Gamma-Emitting Radionuclides by Graded Filters*, Science Vol. 147 p. 290

Uranium particle detection - Sajo-Bohus, L., (1998), Hot Particle Spectrum Determination by Track Image Analysis, Radiat. Phys. Chem., V 51, No 4-6, pp 467-468

Dust sampling for radiation from nuclear weapons testing - Cizdziel, J. V., Hodge, V. F., (2000), *Attics as archives for house infiltrating pollutants: trace elements and pesticides in attic dust and soil from southern Nevada and Utah*, Microchemical Journal 64 85 92 – This study shows the detection of radioisotopes, related to nuclear detonations at the Nevada Test Site, in nearby attic dusts.

Lioy, (2003), *The historical record of air pollution as defined by attic dust, Atmospheric Environment*, 37, 2379 – 2389 – This study shows the steady decline in Cs-137 concentrations in attic dusts since the cessation of atmospheric nuclear detonations.

Dust sampling for uranium particles, with SEM/EDS detection - Parrish, R. R., (2008), *Depleted uranium contamination by inhalation exposure and its detection after 20 years: Implications for human health assessment*, Science of the Total Environment, 390, pp. 58 - 68

Dust sampling and sieving - Lewis, Robert G., (1999), *Distribution of Pesticides and Polycyclic Aromatic Hydrocarbons in House Dust as a Function of Particle Size*, Environmental Health Perspectives V 107, No. 9, Sept.

Hot natural particles - George, A.C. et al, Abstract: *Indoor radon progeny aerosol size measurements in urban, suburban, and rural regions*, Aerosol Science and Technology, v 15, n 3, Oct, 1991, p 170-178

SEM Techniques - Utsunomiya, Satoshi, 2009, Dekker Encyclopedia of Nanoscience And Nanotechnology, CRC PRESS, Ch. 110., Environmental Electron Microscopy Imaging, pp. 1 to 10.

Filippidis, Anestis, 1997, *Mineral, Chemical and Radiological Investigation of a Black Sand at Touzla Cape, near Thessaloniki, Greece*, Environmental Geochemistry and Health, (1997), 19, 83-88

Chapter 3
Isolation & Analysis of Hot Particles in Environmental Particulates

Abstract to Chapter 3

Isolation of hot particles from environmental samples requires multiple steps to collect, separate, and analyze radioactive particulate matter, (RPM). Hot particles contain greater radioactivity than surrounding particles. Samples are collected from media which are high in particulate matter, such as indoor house dusts, dusts from vehicle air filters, household appliance dust buildups, (such as from HVAC coils with forced drafts), vacuum cleaner fine particle traps, and fine sorted surficial soils and sediments.

The steps involved in detecting and isolating hot particles include:
§ Biased sample collection to favor the collection of samples likely to contain hot particles, including field screening of environmental samples of dusts, sediments, and soils by portable gamma spectrometry.
§ Laboratory gamma spectrometry screening of samples to identify signatures for specific radionuclides and total activity of the sample under shielded conditions.
§ Separation of hot particle-enriched fractions via dry sieving and autoradiographic mapping of monolayer preparations of particulate samples.
§ SEM/EDS analysis of selected samples to determine the composition, size, and morphology of individual particles.

Background

The discovery process for hot particles is a series of reductions of inert material while retaining any hot particles. The first step of reduction is done by selection of environmental samples to bias for materials more likely to contain hot particles. This includes activities such as sampling from sites near nuclear material processing centers, and collecting from matrices which are likely to be enriched in air or water deposited hot particles, such as settled indoor dusts and fine sediments. (Due to particle size effects, dust levels typically are enriched in contaminants compared to surrounding soils. ref. Lewis, 1999 and 2002)

Field sieving removed coarse fractions, above 150 microns, which are less likely to carry hot particles. There are fewer processes which create particles of this size, and large dense particles are less likely to travel at modest air velocities. Conversely, finer materials are both more likely to travel large distances by air, and to have higher surface area to weight ratios, allowing for greater adsorption of radioactive materials.

Materials and Methods

The overall sample collection process for this study was biased toward collecting samples of high or low RPM content, rather than random. Environmental sampling is sometimes random, such as in samples collected on a grid-like spatial distribution. Sampling can also be designed to be representative, meaning that a sufficient number of samples has been collected so that a given sample is likely, possibly at the 95 percent confidence level, to be within a given statistical measure of the true central value for an environmental property. Biased sampling is designed, (ref. USEPA 2005), to attempt to use judgments and observations to increase the probability of collecting samples with specific properties. In this case, field sampling was designed to collect candidate samples likely to contain heterogeneously-distributed radiation, as higher-activity individual particles. The biased sample collection method was designed to increase the probability

of detecting hot particles. Conversely, a subset of these samples were selected for comparison from locations which were less likely to contain hot particles.

A limited number of surficial sediment samples had been received in order to collect data on sources of potentially contaminated particulate matter which could contribute to residential dust loading if suspended by winds.

Sites impacted by known sources of radioactive material were selected for sampling. From these locations, sampling methods favored the collection of fine materials. The spatial variability of RPM can be related to its source. In 1949 Hanford engineers detected fallout from the first Soviet atomic bomb test, noting that sampling locations which were separated geographically had similar RPM deposition levels, so long as they shared the same approximate latitude as the test site. (Eisenbud, 1953) In contrast, RPM originating at Hanford is presumed to decrease exponentially with increasing distance from the source, given that Hanford's emissions lack the initial superheated temperatures which result in substantial plume rise for detonation-related particulates.

Reference samples less likely to be affected by HNR, LANL or other recent anthropogenic inputs were collected. A sufficiently large number of samples, (greater than 100 dust samples), was collected to allow for statistical treatment of data.

Sampling incorporates certain judgments about the likelihood of collecting specimens with hot particles. The sampler should be able to hypothesize that a process which can produce dusts exists, and that dust is likely to contain radioactivity. Examples are remediation of sites with radiologically-contaminated soils and sediments, civilian and military nuclear material production facilities, uranium mining operations, fallout from atmospheric weapons testing, phosphate rock operations, air and water erosion of naturally-occurring radioactive mineral deposits and ore bodies, incineration of mixed wastes, and the use of depleted uranium munitions.

Sampling locations were selected which tended to accumulate airborne PM. Care was taken to collect sufficient mass of sample material to analyze for radionuclide content and nonradiation-related characteristics. Locations that accumulate particles include large scale environmental locations such as accretive sediment deposits in river systems and low lying areas which store waters from overland flows. Splash and infiltration zones around rain gutters and low spots in open areas where water is lost to evaporation can accumulate dusts.

Samples were collected from settled dusts in attics and rafters, and dusts brushed from horizontal surfaces. Settled dusts from horizontal surfaces were typically collected from isolated, low traffic areas such as locations under eaves and in basement storage areas. Accumulated dusts were collected from refrigerator coils, ceiling and box fans, dusts from vacuum cleaner bags, HEPA particle traps in certain types of Kelly, Electrolux, and similar canister vacuum cleaners, and dusts from home HVAC systems. Attic dusts were collected from trusses and collar ties to avoid collecting insulating materials. Vacuum cleaner bag dusts and any sediment samples were manually field sieved with a # 100 brass screen, retaining the size fraction below 150 microns. A matched brass cover and collection pan were used with each sieve.

For vacuum bags with multiwalled HEPA filters, the single outer cover was opened, allowing presize-fractioned dusts to be collected. The outer bag dusts generally pass a 150 micron screen, requiring no further separation by sieving. The USA Standard Testing Sieves were purchased from Advantech Manufacturing, (www.advantechmfg.com), and met the ASTM E-11 specification. Sieves, covers, and collection pans were laboratory cleaned using Alconox, ™ and 16 MOhm D.I. or distilled water and air dried. A sufficient number of 150 micron sieves were used so that field cleaning was not required.

Settled dusts and impacted dust samples are subjected to natural sorting processes. Airborne transport processes are limited in the size of material which may be transported, due to the relatively lesser settling velocities of fine particles. Thus, smaller particles are

more likely to travel significant distances as airborne PM. This is especially true given the high densities of some nuclear materials, such as isotopes of lead, uranium, and bismuth. These higher densities can, all others things held equal, increase PM settling velocities. (Lewis, 1999) Finer materials with their greater surface area to mass ratios, are more likely to contain adsorbed radioactive matter. **(**Englert 2007**)**

Fines were collected from sorted sediments, rather than coarse sand or gravel. As with some dusts, the riverine silts and surface soils were field sieved to pass a # 100 sieve, with 150 micron openings. Sieving removes larger objects from dusts such as insect parts and other biological materials, carpet fibers, hairs, nail clippings and small stones. Accumulated dusts, such as fan blade and refrigerator coil dusts were not sieved, as these normally pass a # 100 sieve completely, or are simply aggregates of dusts which were previously airborne, so that the aggregate components are less than 150 microns in size.

A series of physical separations followed by laboratory evaluations identified samples with hot particles. Any hot particles detected were then characterized by Scanning Electron Microscopy/Energy Dispersive X-ray, (SEM/EDS), analyses.

In addition to nuclear materials processing and disposal, sources of radioactive PM include naturally-occurring uranium and uranium ores, combustion of fuels containing NORM, weapons testing fallout, mining and processing of radioactive raw materials such as uranium, potassium, and phosphorus, civilian nuclear reactor emissions, incineration of medical wastes containing radioactive material, and byproducts of radioactive material processing.

Prior to testing by SEM/EDS, samples were tested by atomic absorption spectrophotometry, (AAS), gamma spectroscopy, total alpha, beta and gamma radiation, and digital optical microscopy. Optical microscopy was performed with an Olympus Model BH microscope and a Moticam 2000 2.0 megapixel USB camera. Samples with higher activities as measured by these procedures, were analyzed by autoradiography. Samples with positive autoradiography results, indicating the potential presence of hot

particles, were then analyzed by SEM/EDS. Autoradiography was performed using Kodak Professional BW400CN C-41 process film. (Compare to Vlasova, 2006, which describes a more complex particle tracking preanalysis for mapping hot particles for the SEM).

FIGURE 3.1: Below, Example of positive detections in an autoradiograph film

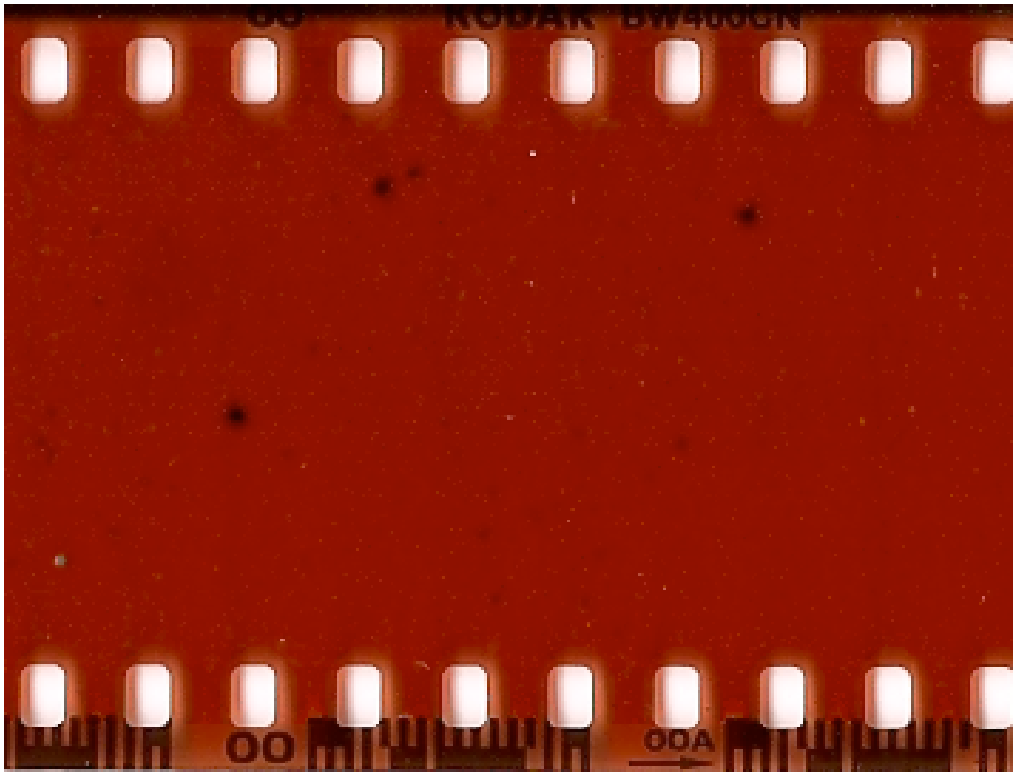

Sampling and Field Analyses

A total of 114 samples of dusts, rocks, sediments, plant materials, and soils were collected in three locations. These locations included two regions where nuclear materials were historically processed, and one former uranium mine.

The first region was Southeastern Washington, in the vicinity of the Hanford Works. Hanford formerly produced nuclear materials for United States atomic weapons

programs. Three subareas were selected for this sampling campaign. The first included Pasco, Kennewick, and Richland, WA. These are the nearest communities to the Hanford Works. A second Hanford region sampling locus was the Yakama Tribal Lands at Wapato, WA, an area which is generally upwind of the Hanford area. The third subarea was centered around Colfax, WA, an area which is generally downwind of the Hanford area.

The second region was the city of Los Alamos and its environs. Los Alamos hosts the Los Alamos National Laboratory, (LANL), a center of nuclear weapons research and development. Samples came from Los Alamos proper and from the Picuris Pueblo, which lies approximately 40 miles to the Northeast of Los Alamos. A small number of samples came directly from process areas of LANL, via dusts collected from the laboratory, or sediments in the laboratory's former WWTP effluent ditch.

The third region was the area around the former Midnite Uranium Mine, in Wellpinit, WA, and the Spokane Indian Reservation. A set of uranium mine-related dust samples was received from the Spokane Indian Nation in Wellpinit, WA. The samples came from structures surrounding the abandoned Midnite Uranium Mine.

The Midnite Mine site is an inactive open-pit uranium mine located on the Spokane Indian Reservation in Stevens County, Washington, about 8 miles northwest of Wellpinit. The mine was operated between 1954 and 1981 by the Dawn Mining Company (DMC) on land leased from the Spokane Indian Tribe. Approximately 2.5 million tons of waste rock, unprocessed, and low-grade ore are currently present at the site. Past mine site investigations indicate that metals, such as arsenic, cadmium, manganese, and uranium and its related decay products have migrated from on-site source areas (i.e., open pits, ore/waste rock piles) into local groundwater and surface waters as a result of acid mine drainage. EPA has conducted a RI/FS that characterizes the nature and extent of contamination both on the site and in nearby impacted areas. (ATSDR 2007)

A small number of additional samples came from accidental radiation release sites,

including a small piece of debris from the, now destroyed, Chernobyl Power Reactor, dusts and sediments from the Mayak Nuclear Works in Chelyabinsk Oblast in south central Russia, and sediment from a suspected nuclear material spill site in the Upper Ganges River basin in India.

Residential dust samples comprised 72 of the 114 samples collected. Home selection was biased in favor of older homes, which may have trapped particulate matter over a longer period than would newer homes. In Richland, WA, many sampled homes were original "A" homes constructed during 1944, expressly to house Hanford's workers. In five locations, dusts were collected from nonresidential structures such as a theater built in 1944 in Richland, WA.

In two instances, soils were collected from residences where dusts had also been collected, to compare surrounding soils to indoor dust matter. Three surface soil samples were collected from locations along the Columbia River adjacent to the former Hanford Uranium Processing Area, a.k.a. the 300 area. Biological samples included two composited samples of lichens, and walnut meats from an orchard on the Columbia River bank opposite the 300 Area.

Samples were collected by manual scraping from dust-covered surfaces. For most samples, the quantity of encrusted dusts was sufficient to produce a dust layer of between 1 and 10 mm thickness, allowing manual removal of dusts with disposable nitrile laboratory gloves, obtained from Best Manufacturing Co. of Menlo, GA. Gloves were discarded after each sample was collected. A 3M P95 particulate removal dust mask was used during sampling, as well as during field sieving of vacuum cleaner bag samples.

Samples were shipped in plastic coolers, with subfreezing temperatures maintained by dry ice for biological samples. Environmental samples were cooled with prefrozen blue ice packs where available. Dust samples were shipped at ambient temperatures.

Samples which were sieved in the laboratory were handled in a laboratory fume hood, with a 50 to 60 fps face velocity. Samples of vehicle air filters collected from employees of the Hanford facility were difficult to handle due to their vary large surface areas and robust construction. The filters were likely to be heavily loaded with dusts, and had total radioactivities which ranged as high as 400 % of background counts, using the portable CdTe gamma spectrometer. (See Chapter 5, sample HR120DZ) These vehicle air filter samples were prepared within a laboratory fume hood.

All vehicle air filter samples were prepared by double bagging each sample, and separating the filter medium from the filter frames, while the filter remained within the plastic bags. The dust was recovered from the filter medium by mechanically tapping the sealed bag and filter on a laboratory benchtop. Dusts removed from the filter were recovered by shaking down any captured particles into a corner of the bag, cutting off this lower corner, and placing the cut end with its dust into a 40 ml precleaned glass VOA sample collection bottle. The radioactivity reported for these samples in Chapter 4 is based on the analysis of particles removed, and not on the filters as a whole. (After removing dusts, the filters counted at background levels, and were not analyzed further.)

Collected samples were double wrapped in low density polyethylene single track Ziploc® bags purchased from S.C. Johnson & Sons. (High water content samples were shipped in Eagle® amber glass 250 ml jars with Teflon seals.) After sealing, each sample bag was screened for total counts using an Inspector handheld digital Radiation Alert Detector® model radiation counter, (a GM tube with 45 mm diameter thin mica window manufactured by SE International, Inc.), as a shipping safety measure. Bagged samples were also analyzed using a portable ICS-4000 gamma spectrometer, manufactured by XRF Corp. of Woburn, MA, to identify any detectable radioisotopes, as an aid in selecting samples for commercial isotopic analyses. The gamma spectrometer was calibrated using a 0.1 uCi Cesium-137 source, and checked with a 0.2 uCi Uranium-238, (depleted uranium), source.

Check samples were collected including reference samples from sites up to 180 miles, or more, distant from HNR. These included dusts thought to be contaminated with depleted uranium and collected from military vehicles used in Kuwait during the first Gulf War and from Iraq, (a source of U-238), vitrified uranium oxide, residential dusts with uranium contamination from Rocky Flats, CO, (both sources of U-238 and U-235), debris from the Chernobyl, Ukraine power reactor, (a source of Sr-90 and Cs-137), sediments and dusts related to a thermal plutonium explosion in Chelyabinsk Oblast in the former Soviet Union, (a source of Cs-137, Pu-239, and Co-60), Ganges River sediments from Northern India, (a source of natural monazite, uranium, and a possible source of Pu-238), and dust and sediment samples from sites surrounding the Los Alamos National Laboratory in Los Alamos, NM, (a source of Th, U, and Lanthanides).

Matches to library spectra were determined by XRF's internal software and were noted in the field notebook.

There was no opportunity to perform field gamma analyses with shielding, nor were background spectra collected at all sampling locations, thus no conclusions were drawn from these field data beyond their use in identifying radionuclides for further analyses by commercial counting facilities.

Gamma spectrometry analyses were repeated in the laboratory at the WPI Department of Civil Engineering, using a second ICS-4000 unit. The persistent thorium emissions seen often, but not always, in field screening, were not seen under these conditions. The initial thorium-positive screening results may have been related to nonsample effects, such as instrument contamination.

As a small grant was available for outside analyses, several samples which had initially shown thorium emissions, were sent to an outside laboratory, PACE Analytical/Walter Miltz Laboratory of Greensburg, PA, for thorium isotopic analyses, and for I-129, a moderately long-lived gas known to sorb to PM. (Nussbaum, 2008)

Two samples of environmental materials contained levels of radioactivity at levels which approached levels of regulatory concern. The State of Washington was notified of a thorium level exceeding 5 pCi/g in silt sampled at Richland, Washington. The New Mexico Environment Department and Los Alamos National Laboratory, (LANL), were consulted on a high beta-activity sample from Acid Canyon in Los Alamos, New Mexico. The Richland sample was of Columbia River sediment with greater than 50 pCi/g of thorium alpha activity. The Los Alamos sample showed greater than 120 pCi/g of beta activity, and the presence of Cesium 137 as determined by gamma spectrometry.

All available data on each sample was forwarded to the appropriate agency. A split of the Acid Canyon sample was forwarded to a contract laboratory engaged by LANL, and quantified at LANL's expense. Both of these samples yielded hot particles for analysis by SEM/EDS, and are described further in Chapter 4, Results and Discussion. Two additional samples of silt were collected. One 50 river miles upstream on the Columbia River, but still bounding the nuclear reservation, and one an additional 35 miles upstream.

Isolation of hot particles from nonradioactive matter

Given the very small fraction of particles with elevated radiation levels, a series of steps were required to identify individual hot particles. The following general separation scheme for hot particles was developed. The sequence of steps used to isolate and analyze hot particles follows after the biased sample collection methods which increase the probability of detecting hot particles. The sequence is:

Collection in of fine solids near known sources of airborne RPM
Sieving to retain < 150 um fraction from dusts, silts, and soils
Nonradiation-based screening analyses
Gamma spectral screening to identify radionuclides and total activity
Autoradiography to confirm and locate hot particles in sample
Analysis by SEM / EDS
Calculate hot particle activity as percent of total sample activity

Sample Preparation

Samples, not already field-sieved, were sieved to pass a 150 micron screen. Samples with high water contents, such as sediments, were dried at 104 degrees C prior to sieving.

Some samples, such as HVAC and vehicle air filters, had too little particulate mass to be sieved. Air filters were collected from locations likely to intercept radioactive particles. These came from sites directly adjacent to HNR and LANL processing areas, or from motor vehicles. Additional air filters were collected from residences. These samples were mechanically agitated in a sealed poly bag. Dust samples were then removed from the bags for analysis. The finest-appearing particles of dust samples were found to attach to the poly bags that contained filters with dry loose dusts. These "sticky" dusts had the appearance of materials which might be attracted by static charge. The attached particles were directly transferred to double-sided taped SEM posts, by pressing the double sided tape-coated posts along the dust-coated poly bag's interior surface.

Some samples came from collection points situated so that only airborne PM was accumulated. These locations included HVAC equipment coils and filters, and residential fan blades and grills. These samples were not sieved, as their particle sizes, when reviewed by optical microscopy and by SEM, were generally below the 150 micron threshold.

Chemical Quality Analysis of Prepared Samples

Particle size - For Fallout, particles are typically less than 1 micron in size, (Shleien 1965), and spherical in shape. (Eisenbud 1953).

Metals content – The nonradioactive metals contents of Region I samples was determined by AAS at the WPI Water Quality Laboratory. Aliquots of 0.35 g to 2.0 g from each sample were nitric acid digested for analysis of metals using a Perkin Elmer AAnalyst

300 Atomic Absorption Spectrophotometer, with an air/acetylene sample excitation system. These digested samples were analyzed for total uranium, cadmium, potassium, chromium, zinc, lead, copper and zinc. Nonradioactive metals were tested to determine whether there were any associations between these metals' concentrations and radionuclide contamination. Certain metals, such as Be, Ni, Ti, and Cr are associated with processing of materials in the nuclear fuel cycle. The intent was to use AAS analyses to quantify metals associated with the nuclear process in order to identify candidates for the more costly and labor-intensive analyses via SEM/EDS.

Total analysis of potassium, uranium and thorium by AAS was proposed to identify samples with higher levels of these, often naturally-occurring, radioactive isotopes. However, the air/acetylene/AAS method did not produce measurable absorbance in prepared uranium standards. ASTM methods for the Analysis of Water and Wastes recommends nitrous oxide/acetylene excitation, but this equipment was not available.

Difficulties in acquiring other necessary equipment, such as a thorium AAS lamp, have delayed U and Th total analyses beyond the required timeline for this project.

Like uranium and thorium, potassium is a component of naturally-occurring radioactive material, (NORM). Total analysis of potassium was within the capability of the AAS method. The average potassium in dust concentration of the Hanford sample set, (n = 12), was 3140 mg/Kg. Given the 0.0117 percent abundance of radioactive K-40, the average dust potassium 40 concentration was 0.37 mg/Kg. The assumes no variance from normal background abundance. At a specific activity of 7.1 uCi/g of K-40, this yields 2.6 nCi/Kg of dust, or 2.6 pCi/g of dust. At this activity level, potassium is responsible for a significant fraction of background activity in the sample set. (Potassium conversion data: K-39 = 93.3 % abundance, K-40 = 0.0117 % abundance, specific activity = 7.1 uCi/g = 7.1 nCi/mg, K-41 = 6.73 % abundance, reference, Argonne NL potassium factsheet) For samples with elevated levels of K-40, as determined by gamma spectrometry, total analysis by AAS is a useful method. It provides additional data on

whether K-40 activity is a result of hot particles enriched in K-40 over other isotopes, or if it results from quantities of naturally-occurring potassium.

Should additional equipment become available, total analyses of uranium and thorium, via nitrous oxide-equipped AAS, would be a useful check on naturally occurring radioactive material in samples, as gamma spectra for the U, Th, Ra, Bi, Po, and Pb series are complex and difficult to resolve due to background interferences in the GeLi and NaI gamma spectroscopy instruments.

Be, Ni, Ti, and Cr were not detected in samples significantly different from levels outside of known source areas for RPM. Other metals were elevated in many samples, particularly in house dust samples. These elevations were not distinguishable from those often seen in urban or areas impacted by nonradiological industrial emissions.

Nonradiological analyses, including AAS, provided limited information regarding the differentiation of samples for hot particle analysis. Resolving the data complexity related to the multiple sources of nonradioactive metals in beyond the scope of this project. Nonradiological analyses were suspended upon completion of these analyses for the Region I, (Hanford, WA), samples. The exception is that total potassium analysis by AAS may provide further data when K-40 is detected by radiological means.

Optical microscopy - Samples were screened by digital optical microscopy for nonsoil particulates such as spheres, needle-like materials, metals, flakes, and other similar artifacts.

Radiation Measurements of Prepared Samples

Upon return to the laboratory at Worcester Polytechnic Institute samples were reanalyzed using another ICS-4000 gamma spectrometer unit with associated local background spectra and a 11 Kg copper-shielded sample well.

Ten additional subsamples were analyzed by PACE Analytical laboratory for Cesium 137, Uranium isotopes, Thorium isotopes, and Iodine 129.

Samples with concentrations of uranium, thorium, or potassium, which differed most from the mean values of each metal for this sample set were analyzed by SEM/EDS for individual high-radionuclide content particles.

Given the high number of particles requiring review by SEM/EDS, autoradiographs of tape samples of dusts were produced to help locate SEM targets. Autoradiographs have been used to visualize radioactivity in natural and biological materials. (Hamilton, 1966, Stover, 1972, Lang 1995) Dust sampling (Eisenbud, 1963 p. 367) and autoradiographs of dusts related to nuclear weapons testing fallout have been used in environmental radiation surveillance. H. M. Clark of RPI, writing for Science in 1954, described a singularly high-level dust fallout pattern around Troy, NY which rained out 36 hours after an April 25, 1953 Nevada Test Site detonation. Clark prepared autoradiographs of paper, wood, asphalt shingles, cloth, and leaves, using 24 hour exposures of X-ray films. Clark described finding uniform circular spots on his films, along with some irregularly-shaped exposed areas.

Autoradiographs were prepared using 400 speed black and white silver halide film and processed normally. Sections of tape with autoradiograph features were forwarded for review by SEM/EDS.

These multiple analyses were designed to identify potential SEM/EDS targets, and to identify homogenous sources of radioactivity in dusts such as naturally-occurring uranium and potassium, which might interfere with searches for infrequent, high-concentration, radionuclide-containing particulates

The sample screening process moved from metals analyses and total counting data to gamma spectrometry using NaI and GeLi detectors at WPI's Physics Dept. Gamma spectroscopy analyses were performed with an XRF Corp. ICS-4000 unit with a

directional CdTe detector, scanning the range from 10 to 2060 keV. Samples were counted using an 11 Kg copper shield. A total of 60 scans were completed. In addition, an EG&G NaI gamma detector and Canberra 727 shield, and an EG&G GeLi nonintrinsic detector with Canberra shield were used in cooperation with the Dept. of Physics at WPI.

Total counts and nonradioactive metals analyses did not prove as effective a means of selecting samples for SEM analyses as gamma spectrometry. NaI and GeLi detectors give information on the nuclide identities which is lacking in gross counts. The NaI detectors provide excellent sensitivity and low background noise for determining which dust samples have higher specific activities. The GeLi detector suffers from a high background, but has excellent energy resolution for detecting low energy gamma emitters such as plutonium.

Autoradiography and SEM/EDS analyses

A LEO/Brucher SEM/EDS system, using a lithium drifted silicon semiconductor X-ray detector, was used for the electron microscopy analyses. All SEM/EDS analyses were performed at Microvision Labs of Chelmsford, MA, a commercial microscopy laboratory. A subset of the samples from LANL, Hanford, and the uranium mine samples, have been reviewed by SEM.

Autoradiography results have proven very effective in selecting samples for SEM analyses. These have the advantage of showing whether hot particles are present, of mapping these particles directly, and allowing a count of hot versus inert particles. Using a set of wide field SEM posts from Microvision Labs, dust and silt samples are prepared by coating these metal posts with a single layer of particles, and exposing these surfaces to high speed photographic film in a dark cabinet for 14 days. The posts can then be directly analyzed, using a scan of the developed film as a guide to locating hot particles.

The electron beam current is 0.60 nAmperes, accelerated at a voltage of < 0.5 to 60 keV. Secondary electrons ejected by surface atoms are detected for imaging. Backscattered

electrons are detected and provide imaging contrast determined by the atomic number of the nuclei with which it interacts. Characteristic X-rays are emitted by ions in excited states created by interaction with the electron beam. These characteristic X-rays are detected by the lithium drifted silicon detector.

Using autoradiography and gamma spectrometry, twelve samples were analyzed by Scanning Electron Microscopy/Energy Dispersive X-ray analysis. These include samples of thorium-containing silts, a layer of what may be evaporite mineral found on rhyolite bedrock in the LANL former WWTP effluent ditch, various air filters used at and around the Hanford Nuclear Reservation and LANL, and dusts from vacuum cleaner bags. Bulk dust samples were sieved, and the fraction passing a #100 sieve was retained.

SEM stubs were prepared on 25 mm diameter aluminum posts, using double sided adhesive tape to retain dusts. Tapes were provided by 3M, (Scotch permanent double sided 0.5 inch, ASTM D-4236 compliant tape), and Ted Pella, Inc., PELCO tape tabs, 25 mm OD.

Bismuth and lead were the primary, but not only, set of hot particles in this dust sample. Rare earth particles, (REE), containing uranium and thorium-based, (U-Th), particles were also present. Similar REE particles were found in many or the dust and sediment samples collected at the HNR. These U-Th particles show remarkably similar spectra demonstrating the presence of cerium, neodymium, samarium, and lanthanum, along with calcium and phosphorous.

A second set of ten samples was prepared in the same fashion. The samples consisted of fines separated from uranium-bearing sediments, collected from the Upper Ganges River headwaters in India. The sample contained large numbers of U-Th rare earth particles, as seen at HNR. Both the HNR and Ganges River samples contained bismuth-lead particles in the 0.5 to 5.0 micron size range.

FIGURE 3.2: Map of Hanford Nuclear Reservation – large scale view

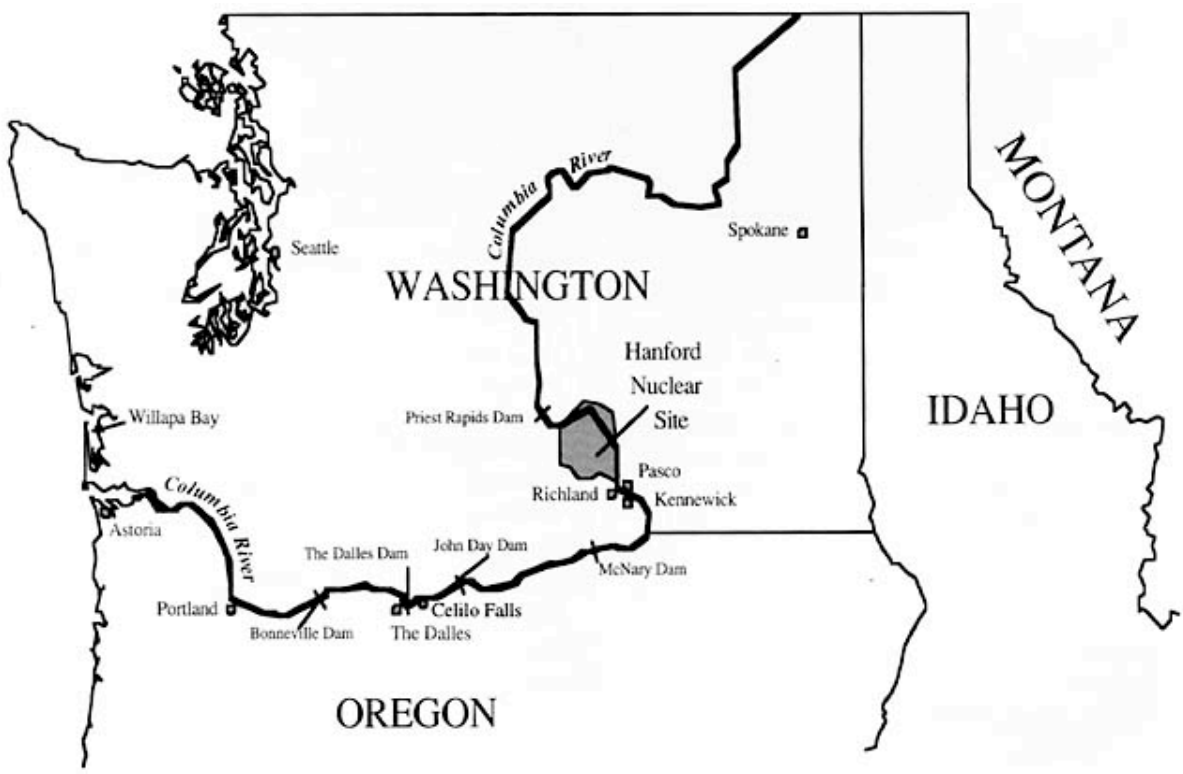

FIGURE 3.3: Map of Hanford, Richland, and Kennewick, WA, showing the site of sample HR091S

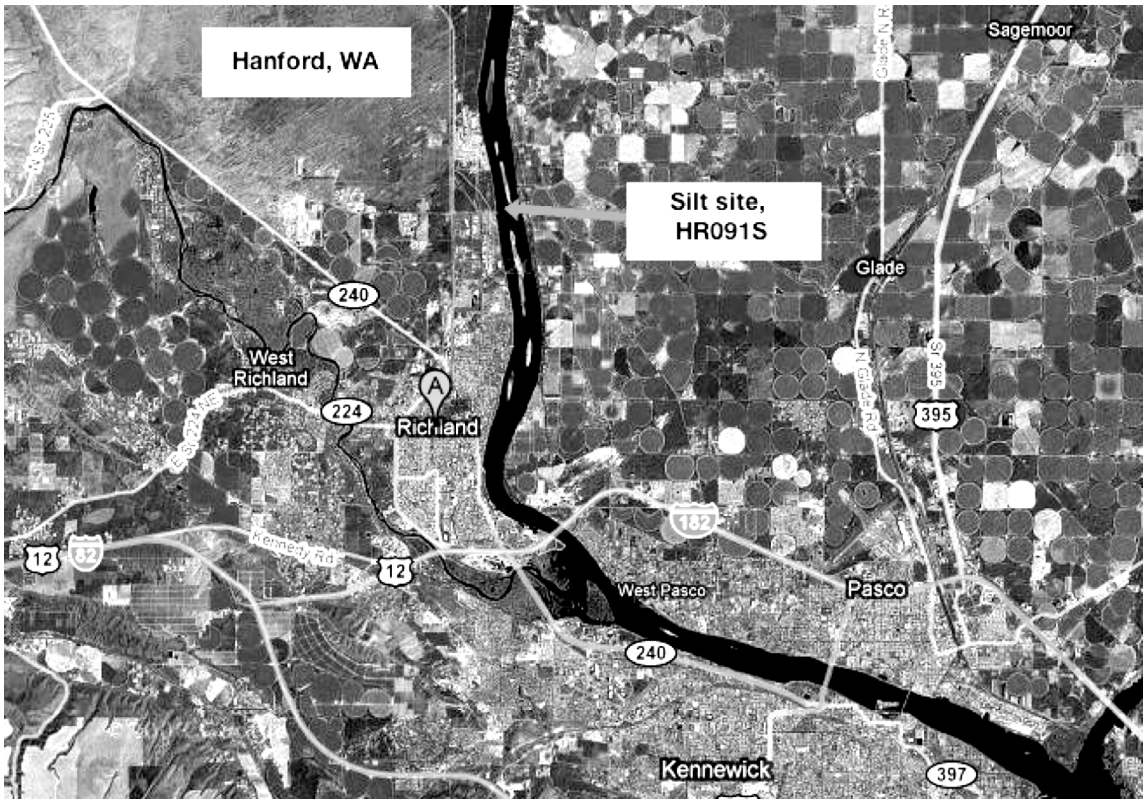

FIGURE 3.4: Below, Map of Los Alamos National Laboratory
Los Alamos, NM

FIGURE 3.5: Below, the site of Acid Canyon sample location LA112S

Methodological Summary

Hot particles were readily captured and detected, using sampling locations which were outside of the perimeter of any actual nuclear facilities.

Biased environmental sampling resulted in the collection of a large set of hot particles. From an initial set of 114 particulate matter samples, 12 samples were carried through a full set of gross radioactivity analyses, autoradiography, and SEM/EDS. Of these, 50 % yielded analyzable hot particles.

High volume air filters which were used as sampling devices, such as automobile cabin and engine air filters, were able to capture hot particles from the environment.

Contaminated surface water sediments, home, appliance, vehicle and clothing dusts, and certain very fine industrial wastes such as coal fly ash, were all ready sources of hot particles.

The fine fraction below 150 microns was most suitable for detecting hot particles.

Autoradiography was successful in detecting hot particles, but required long exposure times.

Chapter 4 – Summary of Hot Particle Detections and Analyses

The initial laboratory procedures were gross chemical and radiological analyses, performed to screen out samples with a low probability of yielding hot particles. Samples were screened for gross alpha and beta activity. Gamma spectrometry gave both quantitative gamma activity data, and qualitative data on likely radioisotopic content.

Nonradioactive analyses were performed, based on the hypothesis that radioactive metals contamination could be related to stable metals concentrations. This was unfounded, possibly because hot particles are driven by dissimilar environmental transport phenomena than those that drive gross chemical contamination. This is another take on the central hypothesis that hot particles are driven by dissimilar environmental transport phenomena compared to gross homogenous radioactive contamination. (This particle vs. chemical quality hypothesis is somewhat of a digression, and is not rigorously treated in this report.)

Metals analyzed included cobalt, copper, cadmium, chromium, lead, and zinc, and potassium, an alkali metal. (Potassium has a naturally-occurring radioactive isotope, K40, which appears, to varying degrees, in most gamma spectra taken from sediment and dust samples in this sample set.)

The results of individual analyses performed follow, along with some brief background on specific measures of radioactivity and radioisotopes.

Commonly-encountered radionucides in this study include radon and daughter products. Naturally-occurring uranium and thorium isotopes were also common radioactive trace components in the set of residential dust samples, as was the more ubiquitous isotope, K40. Lead and bismuth are also an important part of this decay series, and both were found with high frequency. Based on particle sizes, these two elements were found in neat particles which were too large to be associated with radon gas condensates.

Fallout-related isotopes such as strontium-90 and cesium-137, were not encountered as hot particles in the sample set. These are typically quite disperse in environmental samples, and may also be leached, solubilized, or otherwise chemically transformed, making hot particle detection less likely. Co-60, U, and Pu are also sometimes found in fallout, and were also found in dusts and sediments from this sample set.

Process-related isotopes detected in this sample set include U-235 and U-234 at levels exceeding its natural abundance in uranium, Pu-239, Am-241, Th-232, Th-228, Sr-90, multiple lanthanides such as cerium and samariam, and Cd-109.

Note on Background and Units

Activity data are presented in this report as pCi/g, (pico Curies per gram), or in SI units as Becquerels, (Bq). One Bq = 27 pCi/g. Activities may be converted into mass concentrations using the specific activities for each isotope. Conversion of activities to mass concentrations is important to predicting the likely number of hot particles in a sample. (See Chapter 2)

Background, as used in this chapter refers to counts done using an empty sample container, with all other conditions being the same as for counts of samples. Multiple detectors were used, thus sample data is compared only to null counts on the same detector.

Uranium content

Uranium in its natural form is 99.27 mass percent U-238, 0.72 mass percent U-235, and 0.0055 mass percent U-233. Common rock types contain 0.5 to 4.7 ppm total uranium. In natural uranium, U-235 produces 4.5 % of the activity of U-238. High U-235 content, compared to U-238 content, is diagnostic for uranium fuel or weapons activities. Total uranium in samples was measured at the WPI Environmental Engineering Laboratory by AAS. This instrument lacks a nitrous burner assembly, and the attempt to test uranium

by air/acetylene was not successful. Samples were screened using commercial alpha spectrometry, and gamma spectrometry at WPI's Dept. of Physics. Samples which gave positive uranium detections based on gamma spectrometry are noted below.

Some samples were collected specifically to examine any uranium particles present. A set of military helicopter engine air filter dust samples was received from a National Guard unit active in Kuwait and Iraq which was thought to be likely to contain particulate-bound U-238 related to depleted uranium. Depleted uranium has a higher U-238/U-235 ratio, as the U-235 has been removed via enrichment processing. These air vehicles used depleted uranium-based ammunition, and may have been exposed to uranium-carrying dusts. Initial gamma spectrometry results confirmed the presence of low levels of U-238 without any characteristic peaks for U-235. However, given the very low levels of U-238 apparent in the gamma spectra, the characteristic U-235 peaks may also have been below detectable limits. Based on this finding, as well as the low total amount of gamma activity in the sample, the sample was not immediately forwarded for autoradiography testing.

Autoradiographic tests for what appear to be low-value samples may still provide valuable data, but capacity constraints required deferring this set of samples. An additional round of autoradiography tests is underway, including for samples which were less likely to have hot particles, but was not complete at the time of this report.

Samples of dusts from a former uranium oxide mine in Wellpinit, WA yielded total gamma levels at 4.7 times background, with strong peaks for uranium isotopes and uranium decay products including bismuth and thorium. These samples were selected for stage 2 analyses by autoradiography, which found positive detections for hot particles.

One sample, HR084D, dust from the Yakama Nation Environmental Program Office in Wapato, WA, had a U234/U238 activity ratio of 2.6, whereas a typical ratio is close to 1. While total activity due to uranium was below typical background levels, the ratio is similar to that found in fission wastes. Based on this finding, the sample was forwarded

for future autoradiography testing, but was not complete at the time of this report.

Sediment samples collected from the Columbia River in Washington, and the Ganges River in India, both showed gamma spectral peaks due to uranium, These river silt samples are discussed more thoroughly in Chapter 5. Both sets of silt samples were forwarded for autoradiographic analysis.

A sample of house dust collected from a residence adjacent to the Rocky Flats, Colorado, was positive for gamma lines due to uranium. Based on this finding, the sample was forwarded for future autoradiography testing, with a negative result.

Details of the gamma activities of all samples tested are the table, "Results of Gamma Spectroscopy," later in this chapter.

Cesium content

Cs-137 is a common component of fallout from nuclear weapons testing, and a major fission waste product. The absence of this nuclide in dusts with elevated radioactivity may suggest a nonfallout source for that activity. Only one sample gave a positive cesium result. A piece of debris from the control room of the destroyed Chernobyl Unit Four was received from the Russian Institute of Technical Physics. The sample is a piece of the control rod indicator panel cover, and it consists of plastic with a ferromagnetic base material. The debris was contaminated with americium-241, cesium-137, and potassium-40, at approximately 10 times background, based on gamma energy emissions. An optical microscopy review did note that there were a number of particles adhering to the debris. This sample is known to have become contaminated due to the detonation and fire at this reactor, so the transport mechanism is not typical compared to the majority of environmental samples. This sample was archived for future review.

Cadmium 109

This radionuclide is used as a commercial gamma source, sometimes as a replacement for Co-57. Cd-109 was positively identified in sample HR0400D by gamma spectrometry using isotope identification software and a CdTe detector, and confirmed using a NaI detector. This is a house dust sample collected from the an employee of the Hanford Tank Farm. The employee formerly worked on the production line for Cd-109 sources. Total beta counts in this sample were just over one standard deviation above background, or 2 times background the count. Clothing dust can be an important source of secondary radionuclide contamination, and many nuclear facilities do not allow outerwear worn in the workplace to be removed from the jobsite. Likewise accidental contamination victims are normally subjected to a, "strip and ship", where clothing is cut away and disposed of prior to transport for further care. (refs. ATSDR, Cesium Toxicological Profile, 2004, and ATSDR Health Assessment for the Midnite Mine Site, Wellpinit, WA, 2007) Finding a radioisotopic link between the workplace and home could indicate a failure to isolate clothing dust transport from the workplace.

Plutonium

Plutonium in the environment comes as a result of natural fission in uranium ores, weapons testing fallout, Chernobyl fallout, civilian power plant emissions, and weapons processing emissions. Median plutonium-239 activities were 0.35 Bq/Kg, (0.93 pCi/g) in Black Sea sediments, which were subject to both global and Chernobyl-related fallout. (Strezov, 1996) Columbia River sediments upstream of the Hanford Reservation were below 0.012 pCi/g, are presumably subject only to global fallout of plutonium. (Pacific Northwest National Laboratory environmental monitoring data, 2005) Plutonium can also be measured by the ratio of Pu238 to Pu239+241. Typical 238/(239+241) ratios are in the range of 0.028 to 0.08. Higher ratios, up to 0.22, were found for sediments affected by Chernobyl fallout. (as cited in Strezov, 1996)

Several samples collected for this study showed excess plutonium compared to the levels described above. A Los Alamos sediment sample, in a public park, had 38.4 pCi/g total plutonium, well above the medians measured in Columbia River and Black Sea

sediments, with a 238/(239+241) ratio of 0.01, below the typical range. Other Los Alamos soils in the downtown area ranged as high as 2 pCi/g Pu239+241.

Amercium241, a Pu241 decay product, was identified in a sample of debris from the destroyed Chernobyl unit 4 reactor, as well as in the Los Alamos sediment sample described above.

Autoradiography/SEM-EDS identified plutonium particles in worker clothing dust from the Hanford 200 Area. (Sample ID = HR0126DZ) Particle sizes in this sample were in the 5 micron range. Few samples exhibited the presence of hot particles reliably confirmed to contain plutonium. One sample location, the former uranium mine in the Spokane area, had less reliable plutonium detections. These detections were by SEM/EDS only, without gamma spectrometry confirmation. It would be difficult to conclude that the inability to find more samples with hot particles containing plutonium was a definitive analysis of offsite samples, because of the limited number of detected hot particles which could be fully reviewed for this study. Large numbers of hot particles were isolated and detected, far more hot particles were detected than could be fully analyzed by SEM/EDS, because of analytical capacity constraints.

Information about the site where a sample is collected provides some insight on the reliability of the plutonium detections. A potential source exists at the HR0126DZ site for particulate Pu, as Pu is an important component of materials processed in the area where the worker was employed. Such insights do not equal confirmation, but should be considered when reviewing the scope of possible analytical programs.

FIGURE 4.1: Below, SEM/EDS spectra for Pu-containing particles in sample HR0126DZ.

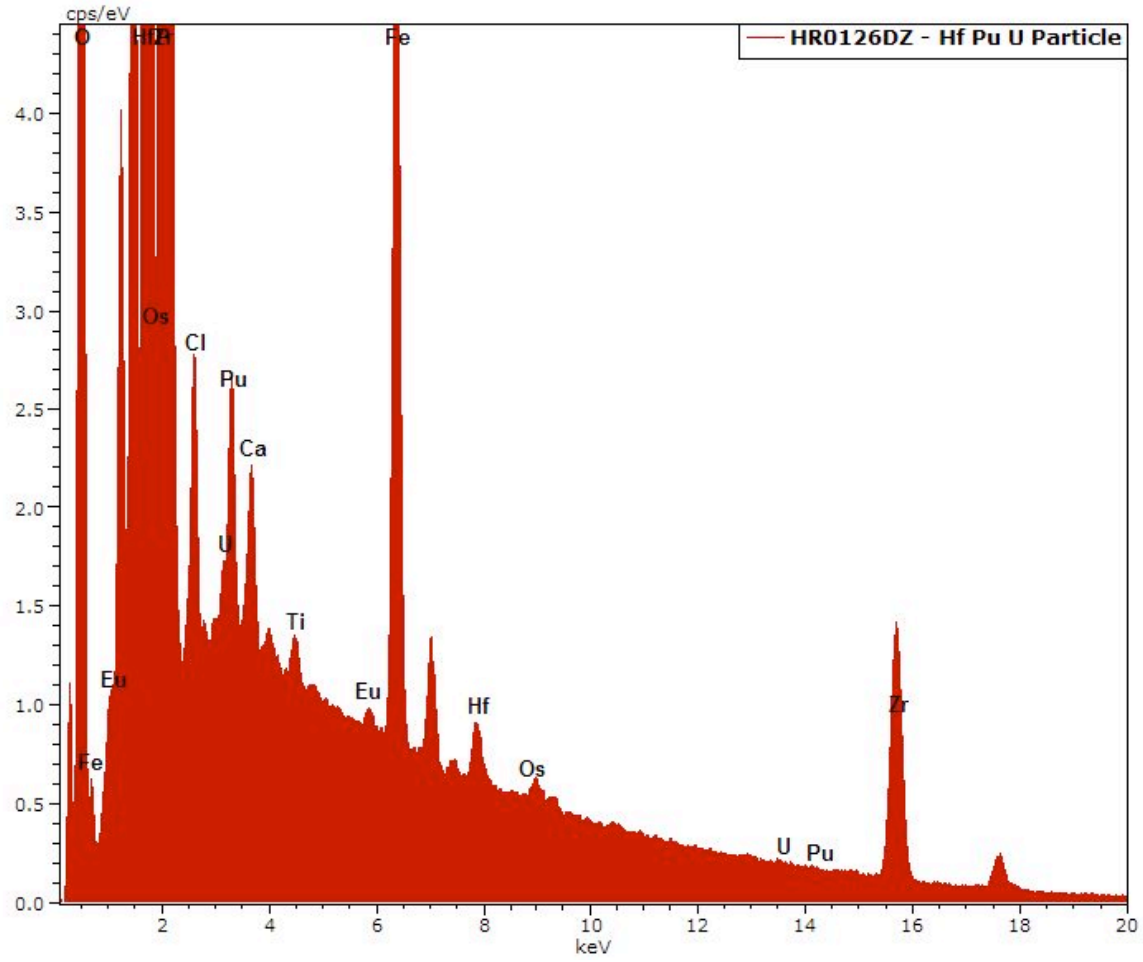

Autoradiography/SEM-EDS did identify two mixed uranium/plutonium particles in a sample strongly contaminated with uranium from the Wellpinit, WA former uranium mine. It is not unheard of to have naturally-occurring plutonium, but it is very rare, to the point that only a single site in Gabon is known to exhibit natural plutonium. (ref. ATSDR Toxicological Profile for Plutonium, 2007) Given the lack of any further corroborating evidence, a future task is to determine whether these isolated Pu particle detections are an instrument error, (such as a peak analysis software problem), an actual detection, or a cross-contamination problem.

Unlike the site where the HR0126DZ sample was collected, the Wellpinit mine is not associated with any known source of plutonium. Further instrumental analysis regarding the Pu "finding" is essential. The SEM/EDS data is not reliable without confirmation.

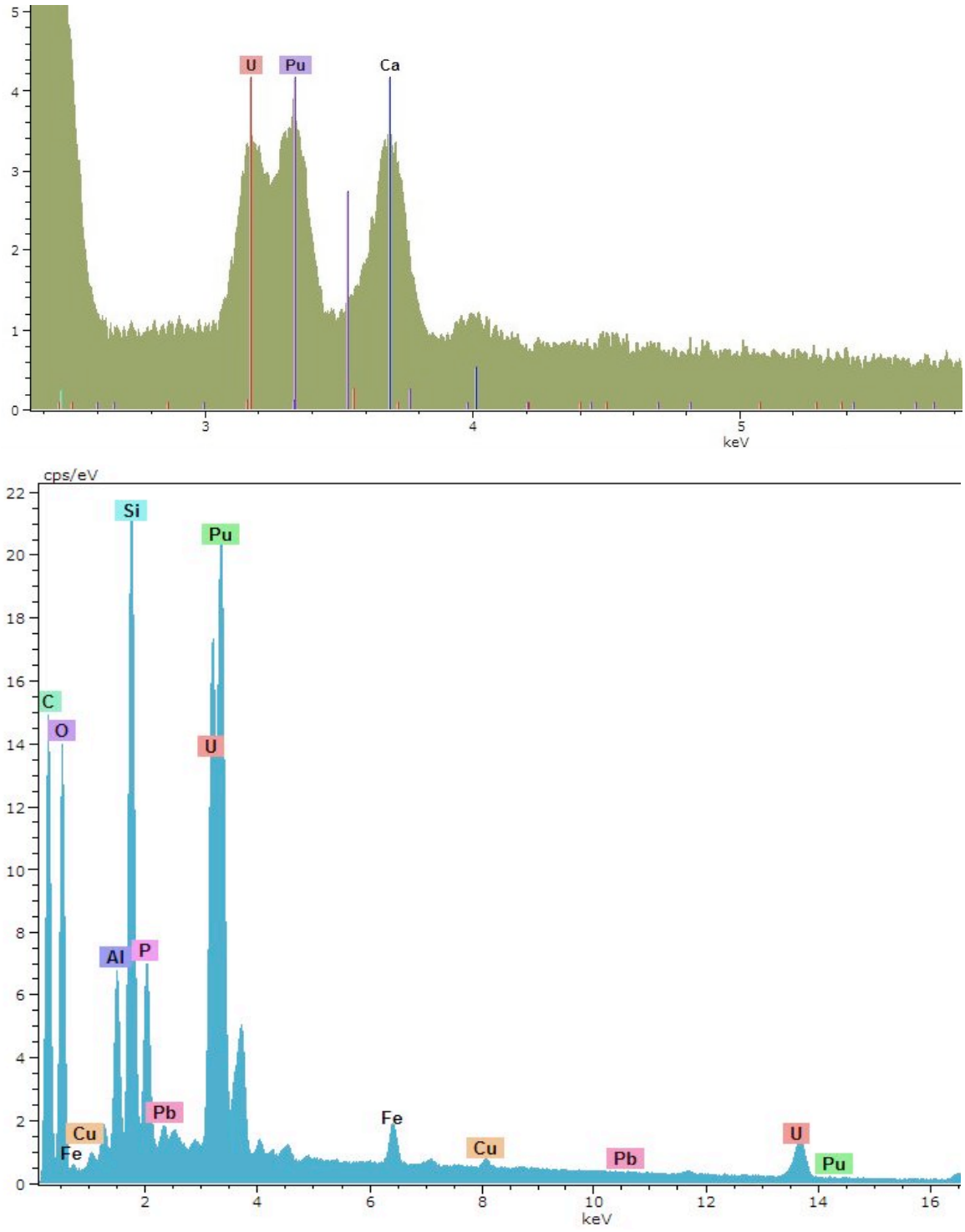

FIGURE 4.2: Above, detail and full view of SEM/EDS data for MMU004D, Wellpinit area uranium mine dust particles showing possible Pu primary spectral lines.

Thorium content

Gamma spectrometry of test samples yielded quantitative results for thorium in multiple samples. Several samples were submitted for commercial gamma spectrometry to quantify thorium and Iodine concentrations. Of three residential dust samples tested for thorium isotopes, one was 30 miles away from HNR at Wapato in the Yakama Indian Nation, one was in Richland 1 mile from the HNR, and one was 11 miles distant, at Kennewick, WA. The results are in pCi/g.

One sample of exposed Columbia riverbed sediment was sieved and the size fraction at 150 um and below was tested for thorium. Based on this test the sediment sample was found to exceed the Washington surface soil concentration criterion for thorium of 5 pCi/g, even when the potential effects of sieving are accounted for. (Sieving may unequally distribute the activity on a weight to weight basis. The sieved fraction actually tested accounted for 45 % of the total sample weight. This would create a 2.2 times concentration factor if the remaining material rejected from this fraction contained no thorium activity.) This data was forwarded to the WADEP, which repeated the investigation.

Aquatic vegetation collected at this location was analyzed by gamma spectroscopy and found to contain a total of 18.4 pCi/g of thorium-228, thorium-230 and thorium-232.

TABLE 4.1: Below, Results of Thorium Isotopic Analyses in pCi/g, PACE data

Location	Richland	Richland	Kennewick	Wapato
Matrix	sieved sediment	dust	dust	dust
Distance from HNR	0.1 miles	1.0 miles	11 miles	30 miles
Th-228	28.6 +/- 7.4	1.0 +/- 0.46	0.98 +/- 0.44	0.37 +/- 0.3
Th-230	9.92 +/- 3.0	1.5 +/- 0.56	0.37 +/- 0.26	0.26 +/- 0.2
Th-232	27.5 +/- 7.1	0.49 +/- 0.37	0.43 +/- 0.25	0.29 +/- 0.2
Total Thorium	66.0	3.02	1.78	0.92

Th-228 is a naturally-occurring thorium isotope in the Th-232 decay series. (Argonne NL, 2002) The Richland sieved sediment sample was further analyzed by autoradiography and SEM/EDS, as the high thorium levels can reflect a greater potential to find hot particles. The samples taken at greater distances were relatively lower on thorium, and were not good candidates for autoradiographic analysis, as it was assumed that the relative number of hot particles in these more distant samples was lower. This sample was found to contain thorium monazites, based on strongly positive autoradiographic analyses, and hot particle detections via SEM/EDS. (See chapter 5 for a detail treatment of these results.) High thorium levels were also found in dusts collected from the Hanford Tank Farm, a high-level nuclear waste holding area, and in sediments collected outside of the Los Alamos National Laboratory. (These results are also discussed in detail in chapter 5.)

Iodine content

Ten samples were analyzed for I-129 content at PACE labs. Two dust samples had traces of I-129, but were below the minimum detection limit. One was dust sample HR0311D from an attic adjacent to the Hanford fenceline. The other was sample HR084D, a bulk dust sample collected from Yakima, WA. Both were in the range of 2 to 3 pCi/g. These were reanalyzed using the WPI Ge-Li detector, however the GeLi detector lacked the needed sensitivity to detect I-129 at the low pCi/g level. There were no dust samples in the study set with positive I129 detections, nor was iodine detected by SEM/EDS. Given that background levels of I129 are in the low pCi/Kg range, (ref. Michel, 2005), a more sensitive analytical method would be required to detect this isotope at typical environmental levels.

Lanthanides

SEM/EDS analysis of a 5 um diameter Fast Flux Test Facility, (FFTF), trailer dust particle contained a mix of cerium 51.5 %, lanthanum 37.7 %, and Neodymium 8.4 %. (Sample 94D) These elements are sometimes found together in rare earth magnets,

fission wastes, and in monazite minerals. The EDS spectrum for this samples was similar to that of the fission waste particles found at the Los Alamos former WWTP Effluent ditch.

Samples of Columbia River sediments and Hanford waste tank farm dust contained these same elements, as well as phosphorous. thorium and calcium and calcium, which are more specifically diagnostic for monazites minerals. Phosphorous, thorium, and calcium were not found in the Fast Flux Test Facility trailer dust particle.

Lanthanide, (rare earth), elements were common among the hot particles detected in this study, and appeared to originate from multiple sources, including sediment cerium monazites, dust cerium monazites, fission wastes, and unidentified sources such as the lanthanide-only particle in the FFTF dust. The lanthanide data is treated more extensively in chapter 5.

Gamma spectra

This method is an excellent screen for SEM/EDS samples, as the total gamma counts per unit time should increase as the total amount of radionuclide rises, and indicates the increasing likelihood of detecting a high level particle. The energy, in keV, of the gamma emissions is a function of the identity of the radionuclide. Note that weights were not standardized. The gamma spectral data is qualitative by isotope, and gives an approximation of the amount of radioactivity in the sample.

Radionuclide identifications assist in the next stage, SEM analyses. In backscatter mode, a high Z detector is used on the SEM. The high Z, (Robinson), detector allows users to separately visualize particles containing elements above a specified atomic number. Radioactive elements identified by gamma spectrometry can be confirmed with the SEM's Robinson detector. The SEM/EDS can not distinguish isotopes having equal numbers of protons, so the gamma spectrometry data is a critical part of the separation and analytical chain for hot particles. Theoretically, the SEM could be operated in

passive mode, (filament off), to gather data on gamma transitions, without a separate gamma spectrometer, but sensitivity is a drawback to such passive mode operation. (See Chapter 6, Future work)

TABLE: The data below are arranged by total gamma counts divided by total null gamma counts. Sample sizes vary from 100g to 1000 mg, so order is not necessarily indicative of specific activity. To the extent that the samples' radioactivity is heterogeneous, the order in the list relates to the total quantity of hot particles in the sample. (This is a simplification, given the size disparities and so on.) The list was produced using CdTe, NaI, and GeLi detectors, thus the need for some level of normalization. The null count in the denominator is respective to the detector used for each sample.

The samples with higher results, (based on SMP to null count ratio or the presence clear gamma peaks related to specific isotopes), from this table were selected for the next analytical step, autoradiography.

TABLE 4.2: Results of Gamma Spectroscopy, total gamma activity and showing nuclides identified

ID	Description	SMP/null	Nuclides detected by gamma spec.
HR0134S	Columbia River sediment	5.5	Th232, Th228
HR0122DZ	Home AC filter Kennewick	4.3	
HR0124DZ	Dust wipe – vehicle	4.1	U235
HR0120DZ	Air filter	4.1	U238 (see fig. next page)
MMU004D	Midnite U mine	3.8	U238, Th232
HR0123DZ	AC filter	3.0	U238, Am241, Pu241
LA101S	Los Alamos downtown soil	1.9	Pu239
HR093D	N. Richland bath vent	1.8	U235
HR0131S	Columbia R. sediment	1.8	Th series, U series
HR097D	N. Richland attic dust	1.7	
LA100D	LANL tech trailer dust	1.6	Pu239
HR101D	Wapato, WA bulk dust	1.6	Ra 226
CHY001S	Chernobyl debris	1.6	Cs137 Np239
Takeda	Ganges R. sed. 0.3 mm	1.5	Th232, U238, Ra226
HR0127DZ	200 Area dust	1.5	Pu239, Th232, U235, Am241

ID	Description	SMP/null	Nuclides detected by gamma spec.
HR311D	404 D Street	1.5	
HR0123DZ	filter – vehicle, coarse only	1.5	
HR0300D	Benton City, WA attic dust	1.5	Th232, U238, U235
HR083D	Seattle reference dust	1.4	Ra226
HR0126DZ	Greenhut dusts	1.4	Th232
Mulberries	N. Richland, 300 Area	1.4	Ra226, Th232
HR092D	Geo. Wash. Way bldg.	1.4	
LA117S	LANL fenceline soil	1.4	
LA120D	Los Alamos Trailer Park	1.3	
HR0105D	Richland "A" house dust	1.3	
HR0132S	Columbia R. sediment	1.3	Th232, U series, Bi
HR086D	Kennewick, WA attic dust	1.2	Th232
Standard	Coal fly ash 1	1.2	* Bi212 Bi214 Ra226 U238
LA109S	Buck, NM Rio Grd. R. sed.	1.2	
HR400D	Worker home	1.2	Cd109
HR412B	Crops, oppo. Richland	1.2	
CO0001D	House dust, Rocky Flats, CO	1.2	U238
LA0112S	Acid Canyon sediment	1.1	Am241, Cs137, Pu, U
HR403D	Richland house dust	1.1	Cs137
HR095D	Richland "A" house	1.1	Th232
MMU002D	Wellpinit house dust	1.1	U238
HR0402D	E of Richland – fire station	1.0	Th232
HR0102D	Yakama house dust	1.0	
Blanks	(averaged)	1.0	
HR083D	Seattle house dust, nonimpact	1.0	Ra226
IRQ05D	Aircraft engine dust	1.0	U238
IRQ01-4D	Aircraft engine dust comp.	1.0	U238
HR0413D	W. Richland "A" house	0.9	U238, U235, Pu239

***** Detections of particles composed solely of bismuth or lead, or a combination of the two, were common to most dust samples, and all coal fly ash samples, and are not indicated in the table. Data from PACE Analytical for a coal fly ash standard material obtained from Microvision Labs of Chelmsford, MA found:

Bi-214	0.94 pCi/g	Bi-212	trace, LT 0.77 pCi/g
Ra-226	0.87 pCi/g	Ra-228	0.89 pCi/g
U-234	0.89 pCi/g	U-235	LT 0.16 pCi/g
U-238	1.17 pCi/g		

Gamma spectrometry yields information on specific energies, (peaks related to a specific radionuclide). The spectra can also be integrated to yield the total gamma activity in a sample. In figure 4.3 below, the area under the magenta curve, (sample HR120DZ), is 4.1 times the area under the blue curve, (blank). (See also, Table 4.2.)

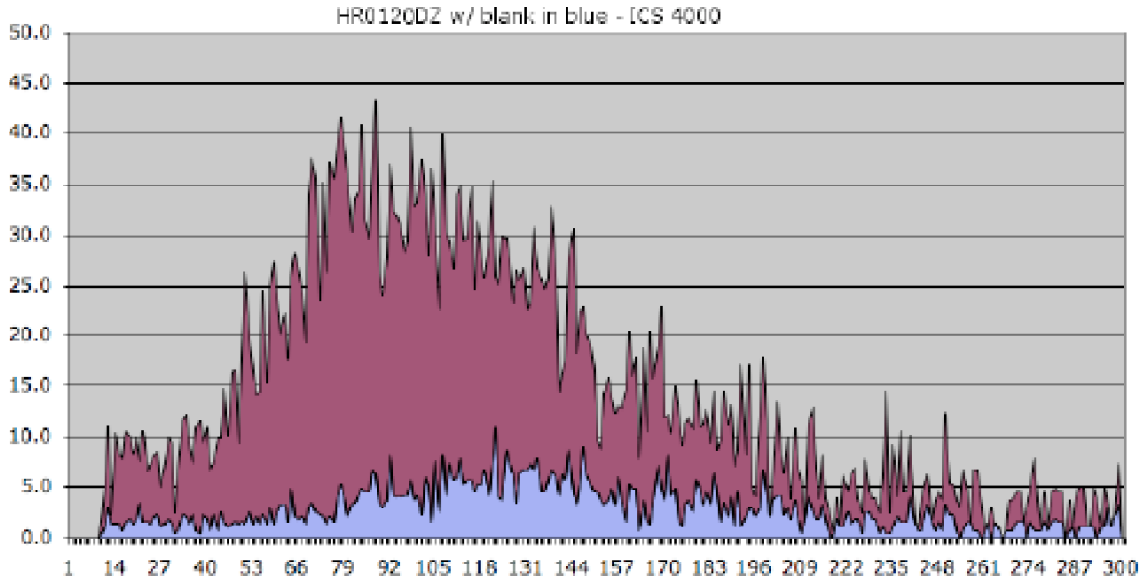

FIGURE 4.3: Above – Blanks, avg., (blue), vs. HR0120DZ CdTe gamma spectrum, (magenta), normalized to identical acquisition times.

Autoradiography

Dust samples with positive gamma spectral results for radionuclides of interest were screened by autoradiography. This technique allows individual hot particles to be visualized by placing unexposed photographic film in contact with a dust sample. Radiation from hot particles exposes film grains in the same fashion as visible photons. Once the film is developed, it yields a map of which areas on the prepared dust-tape contain a hot particle.

Positive gamma spectral results were defined as those with levels substantially above background count levels, or with detectable peaks for plutonium, uranium, cesium, strontium, and similar nuclides associated with nonbackground radiation sources.

Dust samples were prepared as a thin layer of sieved, (passing 150 micron screen), material, directly on 1 inch conducting SEM posts. The dust sample is prepared on double-sided adhesive tape. The posts were mounted on a wooden bar. A two week exposure contact film was made from the posts, using 400 speed color Kodak film. All films were developed commercially. After processing, films and the respective posts were scanned, allowing visualization of developed radioexposed silver grains. Posts with positive film results were then analyzed directly by SEM, with the analyst working from the scanned films to find hot particles. As described by Clark 1953, autoradiographs produced both uniformly circular spots and irregularly shaped exposed areas.

High Z particles were illuminated with a Robinson detector on the SEM apparatus. SEM results are detailed elsewhere in this report.

Autoradiographic and SEM data from this project are consistent with this approach to measuring radiation within samples. Below is a combined image of a cesium-contaminated sample collected from a mineral deposit in the former Los Alamos National Laboratory wastewater treatment plant effluent channel. The film's exposed areas are in the lower right. Exposure time was 14 days. Based on this apparent heterogeneity, this sample was analyzed by SEM/EDS, wherein the presence of heterogeneous radioactivity was confirmed.

The following samples had positive autoradiography results, as defined by the presence of distinct exposed areas on the photofilms. In addition to the seven positive sets of autoradiographs, six were negative, having no exposed areas. Each sample was exposed using at least three 1 inch posts, amounting to >> 10K particles examined per sample.

Positive autoradiographic results

CO001D	Rocky Flats, CO house dust
HR126DZ	Hanford 200 Area – worker clothing dust
HR081S	Columbia River sediment
LA100D	LANL trailer dust
LA112S	LANL former WWTP effluent ditch sediment
MMU004D	Former uranium mine office dust
Takeda002S	Ganges River sediment - fines

FIGURE 4.4: Below – Inorganic precipitate on boulder surface in Acid Canyon, Los Alamos, NM. One of two locations at this site showing a white stain of mineral matter on the rock face, possibly following a former water level mark. This material displays high beta levels, (> 100 pCi/g). This rocky dry watercourse formerly received water waters from the, now closed, LANL WWTP. The 8 inch long portable survey meter at lower left shows the scale.

FIGURE 4.5: Below – LA112S, Los Alamos Acid Canyon sediment, and autoradiograph.

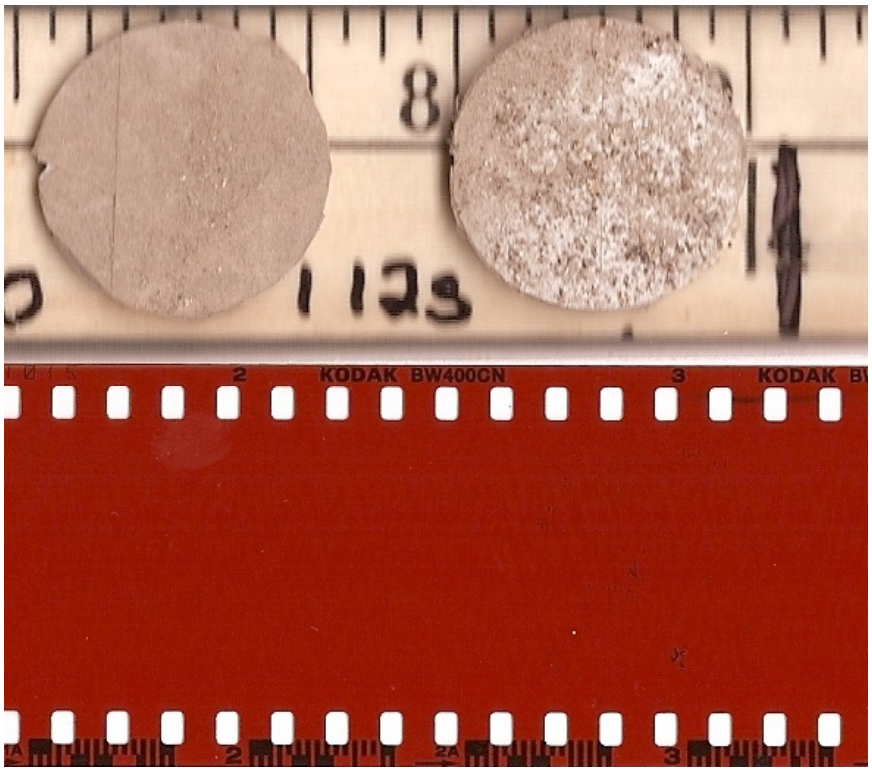

FIGURE 4.6: Below - Thorium-containing silt, sieved to pass a 150 micron screen

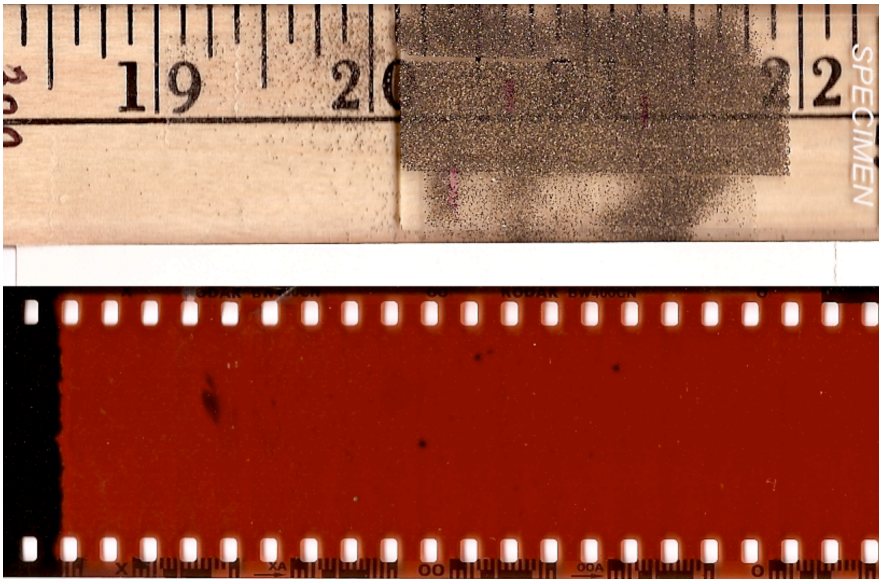

Scanning Electron Microscopy/Energy Dispersive X-ray Analytical Results

SEM/EDS is not a radiographic analytical method. All isotopes with the same Z are quantified together. Thus U235 can not be distinguished from U238, nor can stable Bi be distinguished from radiobismuth, solely through this SEM/EDS. To a degree, hot particle confirmations are inferential, based upon consistency of the detected element with gamma spectral data, particle size and morphology, total elemental composition and inferences which are based on the environmental setting of the samples. This is treated in further detail in chapter 5, which examines the environmental aspects of SEM/EDS hot particle detections. Particles described as "hot" in this study are SEM/EDS detections which were specifically confirmed by gamma spectrometry. Autoradiography also allows the location of hot particles to be accurately mapped on a prepared SEM stub, so that the position data alone could be used to confirm whether a particle consists of stable or unstable, radioactive, isotopes.

Large numbers of hot particles, (>> 100 particles), were detected by SEM/EDS. Most detections were made in using a high-Z X-ray Robinson wide field detector, by scanning a wide microscope field area for a specific element, (such as thorium), and by visually searching for a specific size range or crystal morphology. It was not feasible to quantify the size or elemental composition of each likely hot particle, because of the hourly analytical costs incurred. Alternatively, particles can be visualized by slow scan SEM/EDS, which examines a low magnification image of a layered dust sample, then gives an elemental breakdown for each pixel in the 1024 by 2048 pixel image. Examples of this type of elemental map are given in the following pages, and the appendices.

A short list of some of the hot particles detected is given in the table, spectra, and photomicrographs on the following pages. The table contains examples of primary particle types detected, for illustration purposes. Detected hot particles types which were regularly quantified include, Bi and Bi/Pb, U, Th-lanthanide, Yttrium, lanthanide, Am, Sr, and Cs particles. The bulk of the SEM/EDS data is appended.

A large number of metallic artifacts on the 1 to 10 micron scale are not included. For example a 1930s era newspaper print shop is one of the oldest buildings near the Hanford Nuclear Reservation. Its dust contained large numbers of lead/tin/antimony dusts, which are a breakdown product of corroding printing type.

"Type Blight" is a common form of corrosion of lead/tin/antimony type blocks which may result in the formation of Pb/Sn/Sb dusts. For this sample, the particles contained, Lead 42 to 84 %, Tin ND to 29 %, Antimony 13 to 29 %. The approximate size range was 4 to 40 microns. This structure dates from the 1930's, and was selected as it is the oldest surviving building available to be sampled. These high z particles were confirmed nonradioactive, based on comparison to gamma spectrometry results, and because of inferences which are clear, given the nature of industrial processes at this location.

A more questionable case is a dust sample collected from above the ceiling tiles of the former fast flux test facility security trailer, now a visitors' center located offsite. One 5 um FFTF particle contained primarily an alloy of cerium 51.5 %, lanthanum 37.7 %, and Neodymium 8.4 %. It was approximately 7 um in size. The radioactive nature of this particle was indeterminant, as the small sample size precluded using gamma spectrometry.

Following pages: partial list of particles detected by type, photomicrographs, and SEM/EDS spectral data.

TABLE 4-2: Exhaustively analyzed samples with positive autoradiography, positive gamma spectrometry and positive SEM/EDS results

Particle detected	sample ID	Location	Elements found	size in um
Bismuth	HR0126DZ	Hanford tank farm dust	Bi	1.4
Bismuth	HR0126DZ	Hanford tank farm dust	Bi	0.7
Bi, Pb	HR0126DZ	Hanford tank farm dust	Bi, Pb	2.1
Bi, Pb	HR0126DZ	Hanford tank farm dust	Bi, Pb	4.0
Bi, Pb	HR0126DZ	Hanford tank farm dust	Bi, Pb	0.7
Lead	HR0126DZ	Hanford tank farm dust	Pb	1.2
Bi, Pb	HR0126DZ	Hanford tank farm dust	Bi, Pb	0.7
Bi, Pb	HR0126DZ	Hanford tank farm dust	Bi, Pb	0.7
Lead	HR0126DZ	Hanford tank farm dust	Pb	1.7
Bi, Pb	HR0126DZ	Hanford tank farm dust	Bi, Pb	2.6
Bi, Pb	HR0126DZ	Hanford tank farm dust	Bi, Pb	1.2
Lead	HR0126DZ	Hanford tank farm dust	Pb	1.2
Bi, Pb	HR0126DZ	Hanford tank farm dust	Bi, Pb	2.9
Bi, Pb	HR0126DZ	Hanford tank farm dust	Bi, Pb	1.0
Lead	HR0126DZ	Hanford tank farm dust	Pb	2.4
Bi, Pb	HR0126DZ	Hanford tank farm dust	Bi, Pb	3.6
Bismuth	HR0126DZ	Hanford tank farm dust	Bi	0.7
Bi, Pb	HR0126DZ	Hanford tank farm dust	Bi, Pb	0.7
Bismuth	HR0126DZ	Hanford tank farm dust	Bi	0.7
Bi, Pb	HR0126DZ	Hanford tank farm dust	Bi, Pb	5.2
Lead	HR0126DZ	Hanford tank farm dust	Pb	1.0
Bi, Pb	HR0126DZ	Hanford tank farm dust	Bi, Pb	0.7
Bi, Pb	HR0126DZ	Hanford tank farm dust	Bi, Pb	0.5
Bismuth	LA0100D	LANL trailer dust	Bi C w/ trace Cu O Si	1.6 x 2.5
Lead	LA0100D	LANL trailer dust	Pb w/ Si Ca O C Al Fe Cu Mo	11 x 14
Bismuth	LA0100D	LANL trailer dust	Bi C w/ trace Cu O Si	13 x 20
Bismuth	standard material	Coal fly ash 1	Bi	2
Bismuth	standard material	Coal fly ash 1	Bi	6
Bi, Pb	standard material	Coal fly ash 2	Bi, Pb	2
Bismuth	standard material	Coal fly ash 2	Bi	3
Barium	LA0100D	LANL trailer dust	Ba, S, O, Si, C	3.6

Table 4-2: Continued from previous page

Particle detected	sample ID	Location	Elements found	size in um
Barium	LA0100D	LANL trailer dust	Ba, S, O, Si, C	2.1
Plutonium	HR0126DZ	Hanford tank farm dust	Pu Zr Hf Os Fe Eu U Cl Ca	3.3
U, Pu	MMU004D	Spokane Uranium mine	U Pu Cu Fe Al Si O	20
Th - rare earth	Takeda	Ganges sediment	Th U Ca P La Nd Ce Sm	40 x 60
Th - rare earth	HR0126DZ	Hanford tank farm dust	Th Ce Nd Sm La Y U O P	6.8
Th - rare earth	HR0126DZ	Hanford tank farm dust	Th Ce Nd Sm La Y U O P	10 x 18
Th - rare earth	LA0112S	LANL Acid Canyon	Th Ce Nd SM Nb Al Si Ta	8 x 8
Th - rare earth	LA0112S	LANL Acid Canyon	Th Ce Nd SM Nb Al Si Ta	7 x 9
Th - rare earth	HR0132S	Columbia River silt	Th Ce Nd Sm P O Si Al Fe	95 x 120
Th - rare earth	MMU004D	Spokane Uranium mine	Th Ce Nd Sm La Gd O P Ca Al	80 x 160
Th,Y - rare earth	Takeda	Ganges sediment	Th U Ca P La Nd Ce Sm Y	80 x 120
rare earth	MMU004D	Spokane Uranium mine	Ce Nd Sm La Gd Al SiO P Ca K	25 x 30
rare earth	HR0094D	Expo. trailer, Richland	La Ce Nd Sm Al Si Fe	2 x 4
rare earth	MMU004D	Spokane Uranium mine	Ce Nd Sm La Gd P Si Ca K Y	10 x 14
uranium #1	Takeda	Ganges sediment	U O Si	30 x 20
uranium # 1	MMU004D	Spokane Uranium mine	U Fe Cr Ni	30 x 25
uranium # 2	MMU004D	Spokane Uranium mine	U Pb C O Si Al Fe Mg	12.9
uranium # 3	MMU004D	Spokane Uranium mine	U Pb S O	10 x 12
uranium # 4	MMU004D	Spokane Uranium mine	U Pu Pb Fe Ca Si Al O	4
uranium # 5	MMU004D	Spokane Uranium mine	U Ca Al Si O	3 x 6
uranium # 6	MMU004D	Spokane Uranium mine	U Pb Pu S O	7
uranium # 7	MMU004D	Spokane Uranium mine	U Pu O	8 x 12
uranium # 8	MMU004D	Spokane Uranium mine	U Ca Si Al O C	4
uranium # 9	MMU004D	Spokane Uranium mine	U Ca Si Al O Fe	10 x 15
uranium # 10	MMU004D	Spokane Uranium mine	U Si Al O Pb	5 x 12
uranium # 11	MMU004D	Spokane Uranium mine	U Si Al O Pb	5 x 7
Yttrium	MMU004D	Spokane Uranium mine	Y K Al Si Fe Mn Ti O C	1
Yttrium	Takeda	Ganges sed. – xenotime	Y P Dy O	30 x 30
Yttrium	LA0100D	LANL trailer dust	Y Ti Mn Fe Si O C	1
Zr sphere	LA0112S	LANL Acid Canyon	Zr Si O Ca	33
Nickel tubule	HR126DZ	Hanford tank farm dust	Ni (appears like a SWNT)	10 x 80

An example particle from Table 4.2 illustrates the use of equations noted in Chapter 2. Particle Uranium #1 in sample Takeda.1S is treated as a spherical particle with a radius of 12 microns, containing the radioactive element U. The SEM/EDS data, (see appendix C, SEM/EDS data), shows that this particle is 58 percent, by mass, uranium, and 42 percent, by mass, silicate mineral. This composition is similar to natural uranium in coffinite, and the density and specific activity of this mineral will be used in the solution. (ref. ATSDR 1999, p. 246) Use a density of 12. for the uranium, and 2.65 for the silcate mineral fraction.

This example uses equation 2.5, (Chapter 2), for this one particle,

$$\text{Activity} = 4\pi/3 \sum (\text{area}_j^{3/2} \sum (SA_i \times MF_i \times \text{density}_i)) \qquad (2.5)$$

The area equals: $\pi \times (12.0 \text{ microns})^2 = 452 \text{ microns}^2$

The specific activity for the silicate portion of the particle is zero, so after substituting the area in to the activity equation above, the expression reduces to:

$$\text{Activity} = 4\pi/3 \times (452 \text{ um}^2/\pi)^{3/2} \times (SA_{\text{uranium}} \times 0.58 \times 12.\text{pg/um}^3)$$

The specific activity of natural uranium is the sum of the specific activities of U234, U235, and U238, and is equal to 0.69 attoCuries per picogram. (ref. ATSDR 1999) Solving, the activity is equal to 0.06 pCi.

FIGURE 4.7: Below: Low magnification secondary electron SEM image of silt

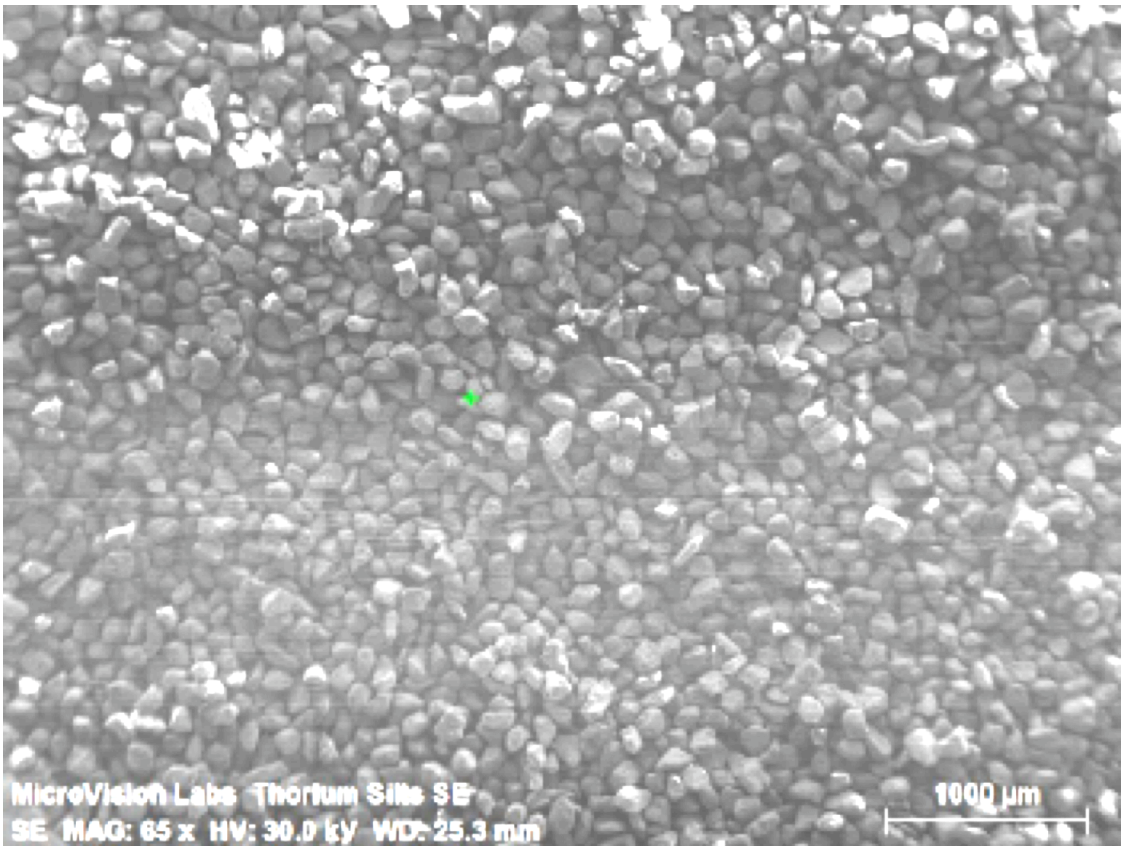

In backscatter mode, high atomic number elements appear as bright locations in the SEM image. In the image below, bright-appearing particles are evenly split in composition between zirconium-based and thorium/rare earth-based grains. Energy Dispersive X-ray, (EDS), spectra were acquired for the thorium containing particles.

Hot particles found in sediments were generally in the 20 to 200 micron size range. Hot particles found in dusts were generally in the 10 micron and smaller size range. This is of public health importance, as this size fraction is designated as, "respirable" since it can be entrained in the lungs.

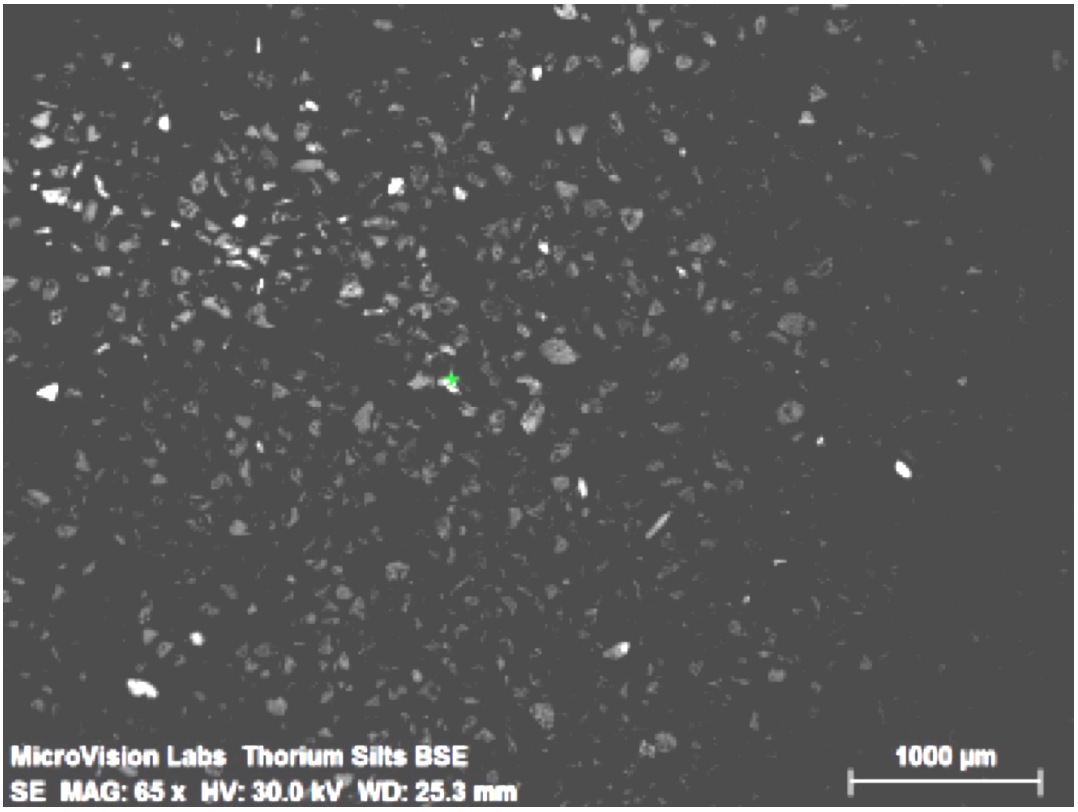

FIGURE 4.8: Above – SEM Micrograph of silt, showing particle in crosshair.

The EDS spectrum, (Fig. 4.9), is shown below for a particle with a high thorium content. The particle selected is indicated above, (Fig. 4.8), in both the backscatter mode and secondary electron mode images, by a green crosshair.

FIGURE 4.9: Below – SEM / EDS spectrum of silt particle indicated in fig. 4.8

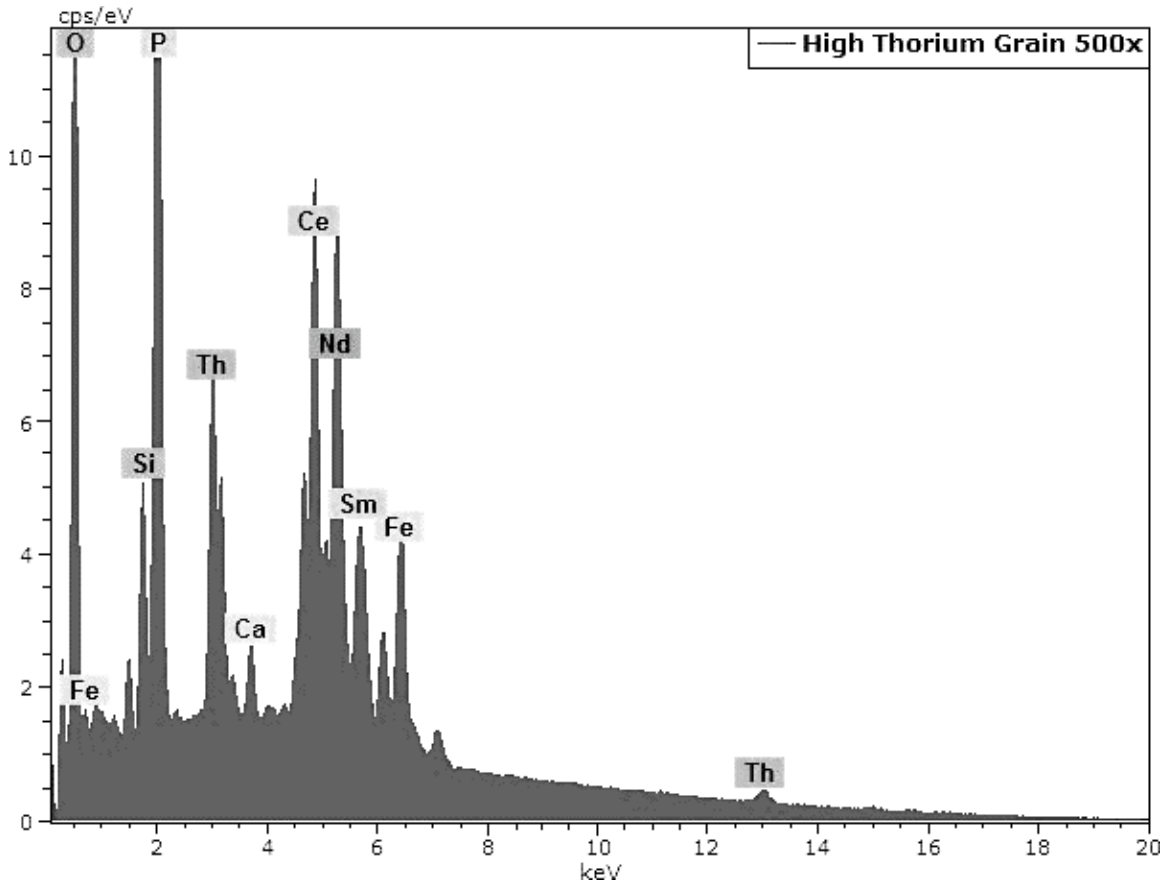

The preceding spectrum, (Fig. 4.9), shows 11.4 % thorium, 19.2 % cerium, 13.7 % neodymium, and 5.7 % samarium. Below, (Fig. 4.10), is an image map showing the distribution of detected elements for one thorium-containing particle and for surrounding Al-Si mineral grains.

FIGURE 4.10: Below – SEM/EDS image element map of thorium silt particle

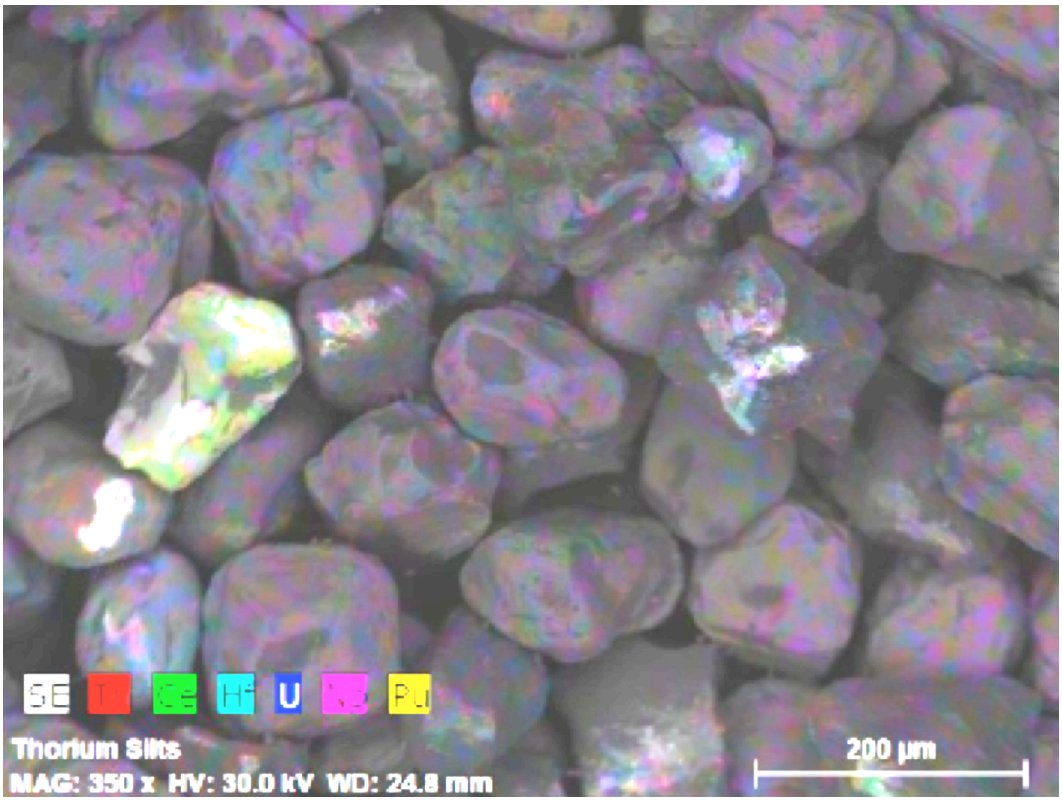

SEM/EDS analysis showed that the average composition of the sample was silica, iron, aluminum, and manganese minerals, and contained 1.9 percent thorium overall. The average composition spectrum is shown in Figure 4.11.

FIGURE 4.11: Below – SEM/EDS spectrum of silt, average elemental composition

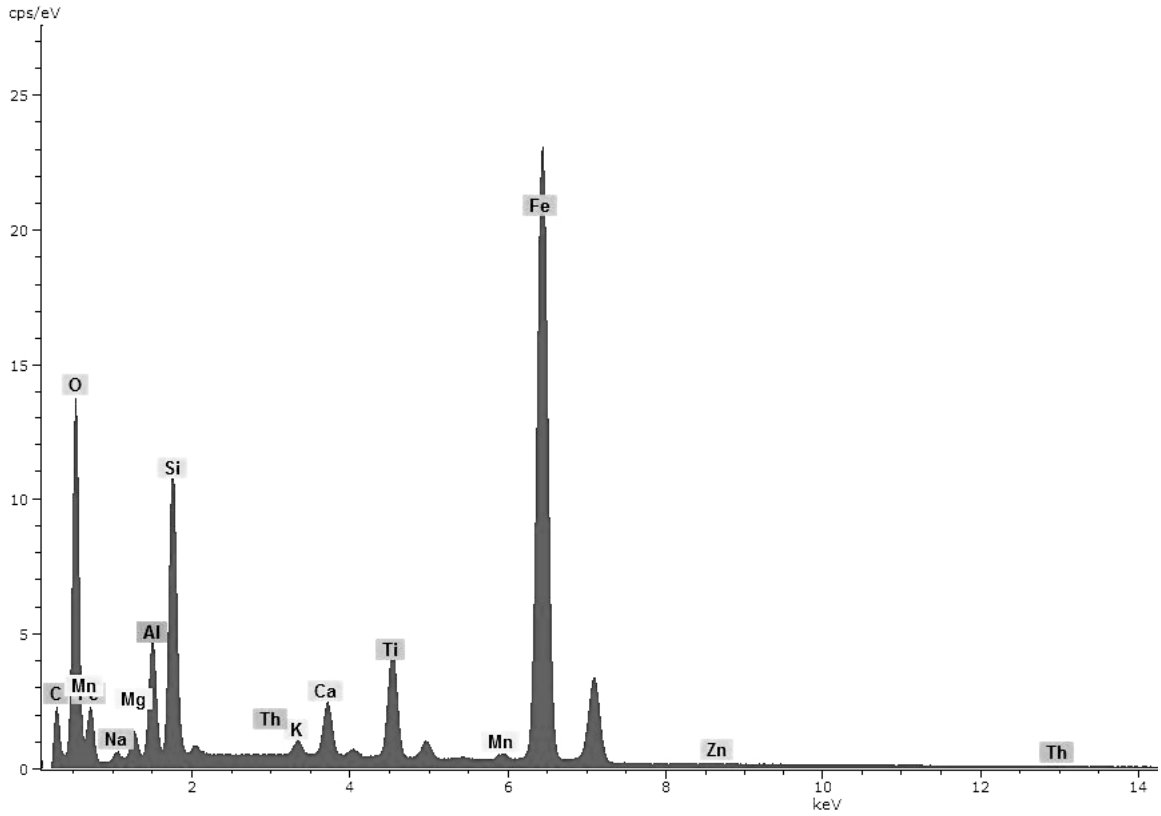

FIGURE 4.12: Below – SEM/EDS spectra of Hanford Silt particle and Uranium Mine Monazite particle, showing similar levels of Th, Ca, P, and Lanthanides in each.

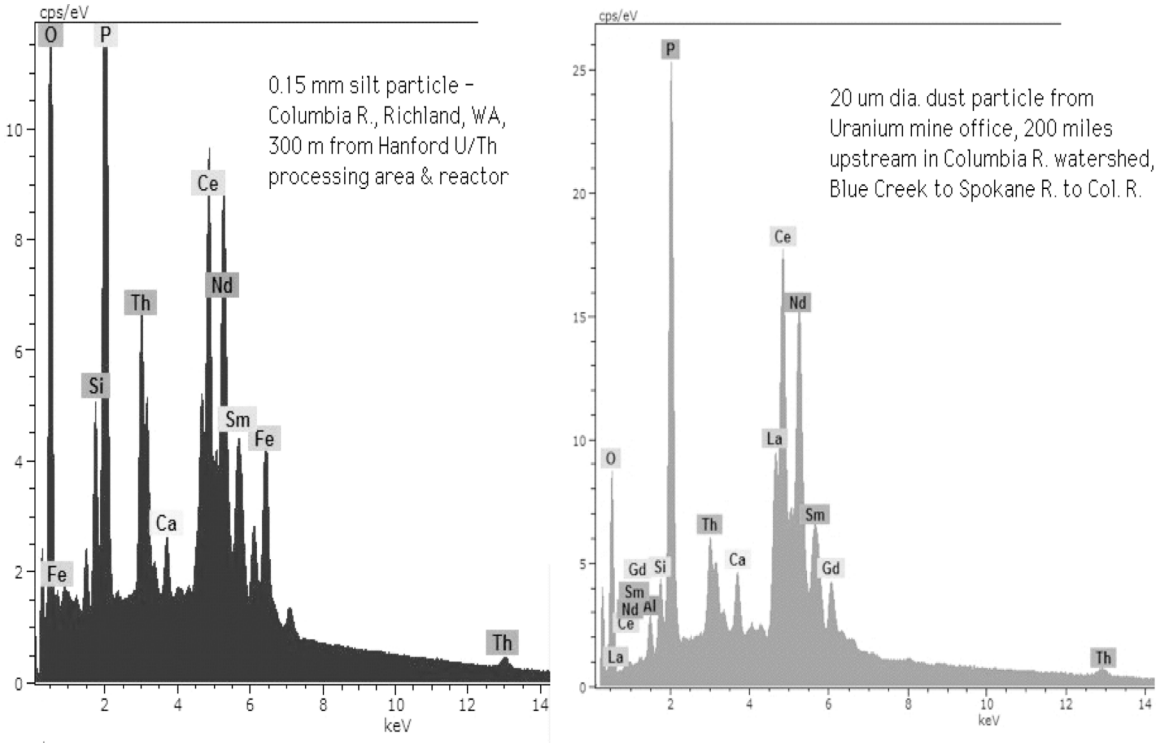

FIGURE 4.13: Below – Detail of U and Pu peak energies from SEM/EDS spectrum shown in figure 4.12, right.

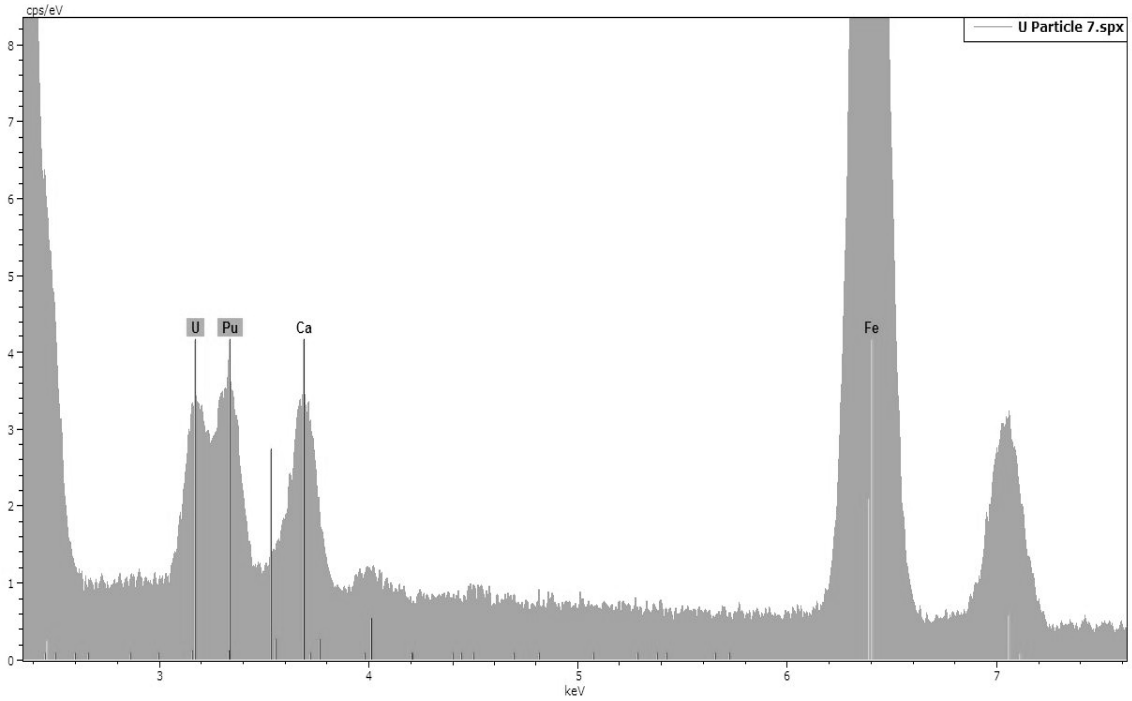

Approximately 0.4 percent of the particles in the sieved Hanford silt sample were composed primarily of thorium, cerium, samarium, and neodymium minerals. Thorium concentrations in this second type of particle ranged up to 11.4 percent. Values for n and N, (see chapter 2, Background), can be obtained by direct counting. The radiographic sample heterogeneity for this sample is 2.2.

FIGURE 4.14: Below – SEM/EDS spectrum of Midnite Uranium Mine monazite particle

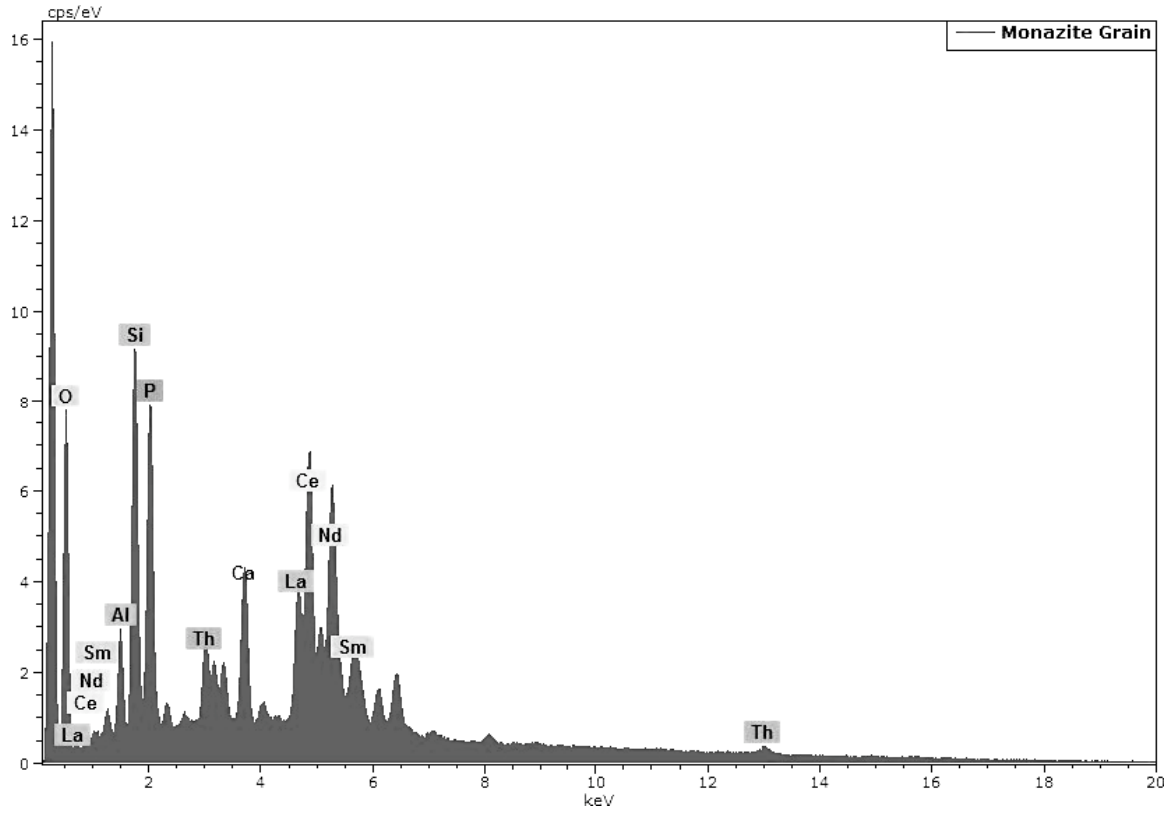

FIGURE 4.15: Below – SEM/EDS spectrum of Midnite Uranium Mine uranium particle

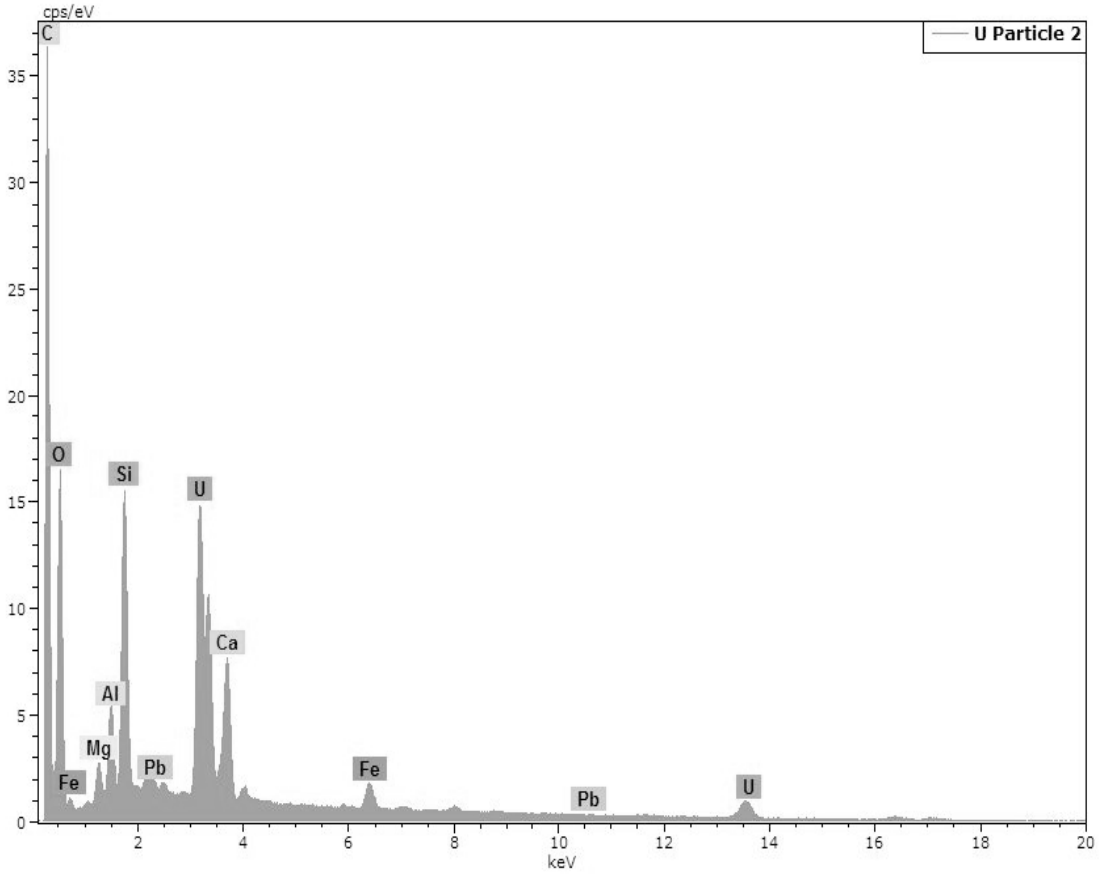

FIGURE 4.16: Below – SEM photomicrograph of uranium and monazite particles from Midnite Uranium Mine dust sample

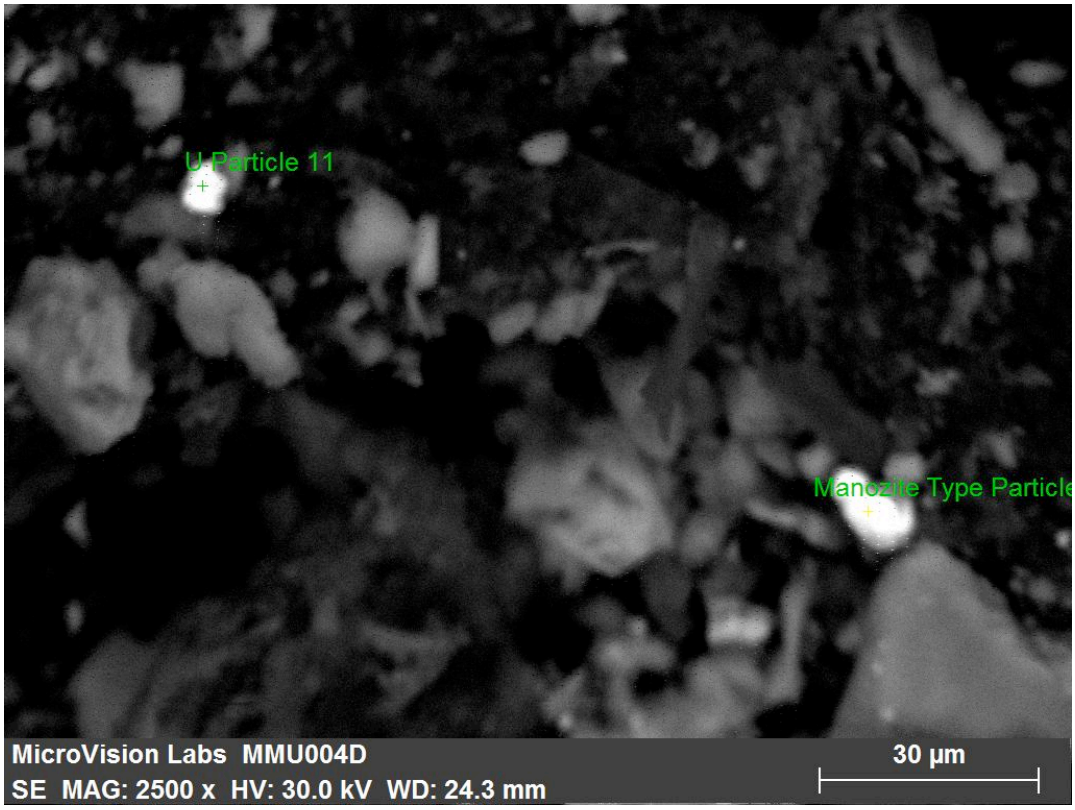

The number of optical microscopy artifacts which are distinct from soil particles is very large, and beyond the scope of this study. These can be related to radioactivity in particles, if any, using quantitative mapping via autoradiography. The optical microscope would then serve as an alternate detector, replacing SEM/EDS, but providing no quantitative data. Optical microscopy was performed on 10 dust samples, however this type of data was too complex and too nonspecific to provide insights into potential hot particles.

Following pages: Examples of optical microscopy artifacts.

Microscopy Results – For illustration only, 4 of 53 micrographs shown.

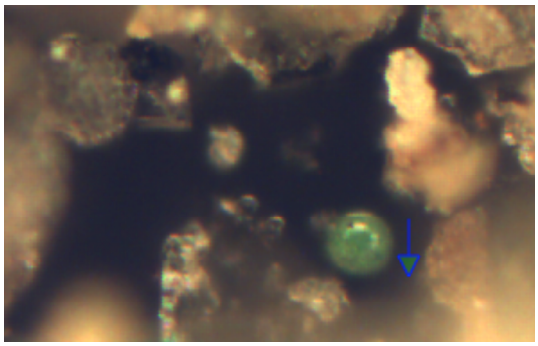

FIGURE 4.17: Above - 20 um green sphere – HR0121DZ –air filter dust

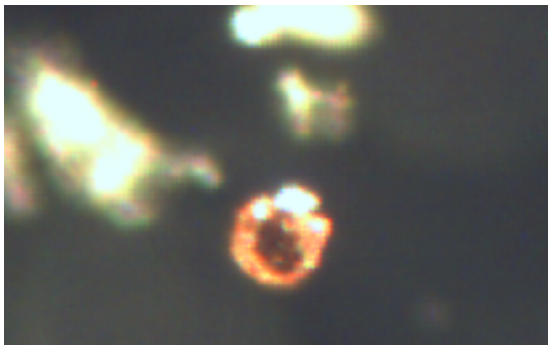

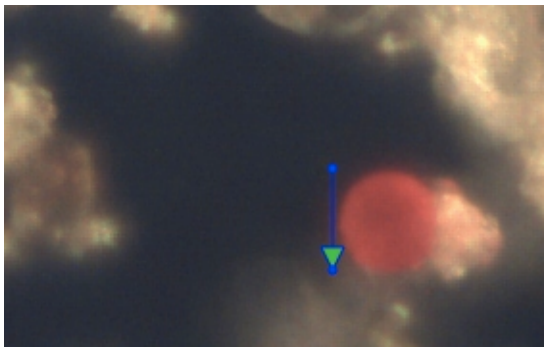

FIGURE 4.18: Above Left, 25 um red sphere – common artifact in vacuum cleaner dust, and in ceiling tile dusts, FIGURE 4.19: Above, right

FIGURE 4.20: Below – Ceiling tile dusts – showing an aggregate of finer particles

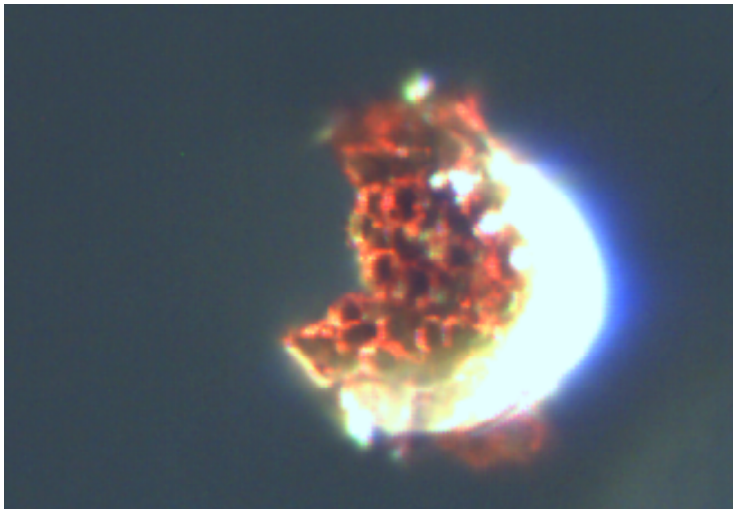

Chapter 5

Environmental Fate and Transport of Hot Particles in Dusts and Sediments

case 1 – Thorium rare earths

case 2 – NORM/ U series, radon and bismuth

case 3 – Uranium mine dusts

case 4 – Ganges river sediments

Abstract

Analyses which focus on hot particles can identify RPM related to specific nuclear processes in samples with gross radiation levels close to background. Analyzing an individual particle overcomes the diluting effects of particle dispersion in the environment. Individual particle analyses have greater sensitivity because no signal is acquired from inert material, as happens with bulk sample analyses. Hot particles are isolated from environmental samples by sieving and autoradiographic mapping. Analyses are performed by gamma spectrometry of bulk samples or sample fractions, while individual particles are analyzed by SEM/EDS.

The SEM/EDS data is compared to known materials from radiogenic processes, based on specific particle properties. Properties measured include particle size, mineral and elemental associations, morphology, and distribution within the particles or bulk sample.

Dusts sampled were generally in a size range of 1 to 20 um. RPM from nuclear test fallout is 1 to 2 um, while radon daughters are nanometer-sized. (reference: McNaughton, 2008)

Dust samples which contained the thorium-bearing mineral, cerium-monazite, as well as uranium oxide particles, had the nonradioactive accompanying elements, P and Ca. The uranium ore, Autunite, formula CaUO2PO4, as found in samples from a Spokane, WA area uranium mine, also contained the elements P, Ca, and Th. RPM found in sediment

samples related to nuclear reactor fission wastes also contained thorium-rare earth particles, but could be distinguished from the monazites, as these particles lacked P, and did have Ta and Pu.

The morphology of RPM was varied within the sample set. Types detected included minerals that were distinguished by their crystalline form, fallout particles which had typically spherical form, and subangular, sorted and eroded sediment particles.

The distribution of RPM within a bulk sample can provide data its origin. For RPM from nuclear fission waste, heterogeneous surficial radioactive deposits were detected as evaporites on mineral substrates.

Background

Gross radiological analyses on environmental samples often detect levels of activity which are close to background levels, even at locations where specific sources of radioactive material release may exist. For example, an earlier study, (Kaltofen 2005), found multiple locations with specific radionuclide contamination. These levels were too close to background levels of radioactivity to definitively assign a potential source for many of these findings. Background levels of radiation can be highly variable, so increased levels of activity beyond the "background" is not necessarily sufficient to identify the origin of that activity.

Radionuclide identity alone is not sufficient to distinguish among potential sources of radioactive material in environmental samples, given that the same isotope can appear in nuclear materials of multiple origins, such as uranium from NORM, civilian nuclear power plant wastes, and fugitive emissions from weaponization of nuclear materials.

This difficulty in fingerprinting is greater when the radionuclide of interest is also one which has a known global component. For example strontium90 in the environment can occur to due the presence of nuclear fission products due to improper waste disposal, and

also from fallout from nuclear detonations. Thorium can be found in fission wastes, thorium fuel cycle wastes, and in naturally-occurring thorium from monazite minerals. Bismuth can be found in nuclear fuel, but also in radon daughters.

When radioactivity exists as RPM, the particles which carry the activity exhibit well-described environmental transport and sorting behaviors. RPM may have higher than average densities, and may be nonconservative due to radiological decay. Nevertheless, these should follow a predictable pattern in the environment. The characteristics of the RPM, such as its particle size, sorting, morphology, and trace components, may also preserve information about how the RPM was formed.

While an environmental sample may be at near-background levels of radionuclides typically found in NORM, such as bismuth and uranium, it may yet be of a specific anthropogenic origin. Physical evidence of anthropogenic origin may be found through isolation and analysis of RPM. For an environmental sample containing background levels of bismuth and uranium, the RPM may be large, (> 10 microns), crystalline rather than spherical, and associated with rare earths and americium. These characteristics are evidence that the uranium is a product of nuclear reactor fission wastes, rather than naturally-occurring.

Case 1 – Thorium-containing particles - Rare earth elements from Monazites vs. Nuclear fission products

Thorium is often described as a natural part of background radiation, meaning radiation which is present independent of anthropogenic nuclear activity. Thorium is a component of the uranium decay series. When thorium is found at levels close to background, it has been reasonable to assume that this is related to thorium's position in the decay chain from naturally-occurring uranium. Alternative sources of thorium exist, such as the thorium bearing mineral monazite, and wastes from the use thorium in nuclear reactors.

Thorium-rare earth particles arise from naturally-occurring monazite minerals and nuclear reactor fission products. At right are photomicrographs and SEM/EDS spectra for six particulate samples. Two are river sediments, (Columbia River Wash. And Ganges R. India), three are collected dusts, (Hanford, WA, Los Alamos, NM, and a Washington Uranium Mine), one is a surficial mineral deposit from a WWTP effluent channel at Los Alamos National Laboratory. Sample total gamma counts range from below background to about 2.5 times background levels. Potential radionuclide source materials were identified in samples with specific activities were very close to background. Monazite materials were identified in five of these six samples. One sample shows discrete, nonaggregated, bismuth particles at 2 um diameter, larger than expected for radon daughters in air.

For one dust sample, which was exhaustively separated and analyzed, the predicted activity from detected hot particles was very close to the total activity of the bulk sample, from which these hot particles had been isolated. This suggests that the procedure should be repeated on a number of samples, to determine if heterogeneously distributed activity can be measured as a percent of total sample activity.

The size and density of hot particles in the environment affects how these particles are transported. Smaller, lighter particles will tend to remain airborne sufficiently long to be transported large distances. Dense materials, such as bismuth, will remain airborne for considerable periods if particle size is sufficiently small. Hot particles of dense, high concentration bismuth and lead were found in this study's dust samples. The size of these particles ranged from 2 to 20 microns.

Larger, well sorted, particles of Th - rare earths were found in river sediment samples. These particles were in the 50 to 150 microns size range, suggesting that had any finer thorium rare earth particles existed originally, these may have remained suspended in the water column, and were not deposited at the same location.

In addition to environmental sorting actions, the processes which produce hot particles

result in specific particle size distributions. Fuel combustion and fossil fuel extraction release large amounts of radon, which produces nanometer-sized radon progeny particles. Nuclear detonations produce hot particles close to 1 micron in size. Residential dusts and dust aggregates are found in the 2 to 20 micron size range. (Lioy 2002, Kaltofen 2005) Sedimentation processes, such as the washout of mine tailings, can be 100 microns and larger.

Dust samples which contained the thorium-bearing mineral, cerium-monazite, as well as uranium oxide particles, had the nonradioactive accompanying elements, P and Ca. The uranium ore, Autunite, formula CaUO2PO4, as found in samples from a Spokane, WA area uranium mine, also contained the elements P, Ca, and Th.

RPM found in Los Alamos, NM Acid Canyon sediment samples related to nuclear reactor fission wastes also contained thorium-rare earth particles, but could be distinguished from the monazites, as these particles lacked P, and did have Ta and Pu. The uranium and plutonium were both confirmed by gross spectrometry. This gross spectrometry also detected strontium-90 and americium-241, two elements which were not seen by SEM/EDS. (Although a number of hot particles in this sample remained uncharacterized due to instrument availability limitations.)

TABLE 5.1: Below - Gross analytical data from sample split between this study and LANL staff, in pCi/g.

Pu-238	0.04	+/- 0.07
Pu-239/240	38.0	+/- 2.9
U-234	9.3	+/- 0.8
U-238	3.1	+/- 0.3
Sr-90	21.4	+/- 2.5
Am-241	3.9	+/- 0.5

Source, 2009 LANL data in pCi/g by Paragon Laboratory, Kaltofen 11/2008 Los Alamos, NM sample

Acid Canyon received treated and untreated wastewaters from research activities related to nuclear weapons. From 1943 to 1951 these wastewaters were untreated. Treated wastewaters were received from 1951, until the WWTP closed in 1964. The effluent received a variety of radioactive materials including tritium, and isotopes of strontium, cesium, uranium, plutonium, and americium. These are the same radioactive materials found in analyses of sediment, as analyzed by gamma spectrometry at WPI, and by LANL's contract laboratory, Paragon. (ref. U.S. Dept. of Energy, 2004)

In the case of the thorium silt sample, air transport of particles of this size may be limited, based on the size and high density of the particle. Groundwater movement would not normally transport an intact particle of this size. Groundwaters can, however, transport dissolved minerals which may precipitate based on changing redox conditions. In the lower carbonate environment of the riverwater, thorium complexed with silicates and phosphates, precipitates as hydroxides. (D. Dunning, personal communication) SEM/EDS data for this sample show that Si, Al, and P were all major components of the substrate minerals at the sample site.

Surface water is capable of large particle transport as suspended or bed load sediment. The rounded shape of the thorium containing particles is consistent with surface erosion related to sediment transport. The sorted nature of the particle sample is an artifact of sieving to below 150 um diameter, and the effects of exposure to the rapid flow of the Columbia River, which may remove fines.

In evaluating the elements found with the thorium particles, it is notable that the rare earth elements detected with thorium in these particles, (cerium, samarium, and neodymium), are consistent with fission products found in spent fuel. (Haggerty, 1983) Historic maps also indicate that thorium rich nuclear fuels were disposed of near this location. A Dept. of Energy workplan for this location indicates that thorium fission product wastes were buried in a floodplain 3000 feet West of this location. (DOE RL-2004-37, "Thoria Trench" area 618-7)

A new set of six samples of the Columbia River silt was collected by the Washington State Dept. of Environment, split, and analyzed by the State of Washington and for this study. Results for this set were lower than the original sample, by an order of magnitude. Upon review of the photographs of the State's sampling effort, one difference between the first and second sample sets, was that the State's samples also included more deeply buried material, rather than the top 1 cm or less, as with the first set. If the excess thorium were concentrated as a surficial deposit, then collecting a thicker sediment profile would result in a lower total thorium concentration. The Th228/Th232 ratios were similar between the two sample sets, at 1.0 +/- 0.2. The total thorium ranged from 2.0 to 5.9 pCi/g for the State samples, and were at 66 pCi/g for the original set. (The State sample were analyzed by ALS Paragon, the original set were analyzed by General Electric/PACE.)

Above: The middle photomicrograph and spectrum shows a particle containing thorium, uranium, rare earth elements, and plutonium, without calcium or phosphorous. These elements are characteristic of nuclear fission products. The sample was collected at Los Alamos National Laboratory's former wastewater discharge channel. At top and bottom are data from particles containing similar elements, but with Ca and P related to cerium-monazite minerals. These particles were collected from Hanford Nuclear Reservation, where thorium processing took place. The particles were isolated from dust, (waste processing area), and nearby sediment, (Columbia River), containing thorium monazite mineral.

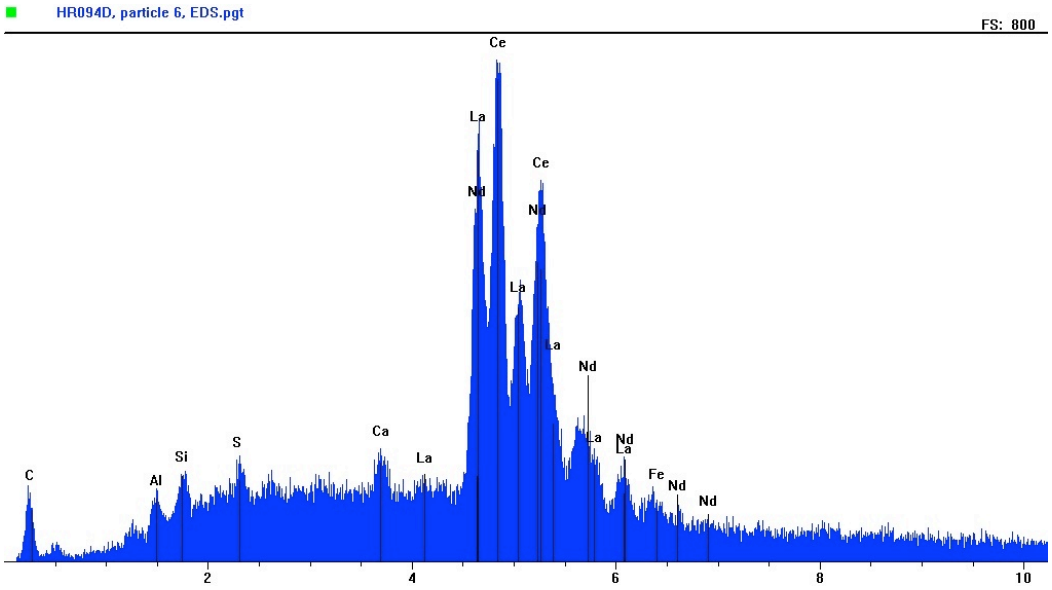

FIGURE 5.1: Above – SEM/EDS spectrum of dust sample HR094D

Dust containing the rare earths Nd, La, Ce, and Sm were found at the former FFTF trailer, (now recycled as a visitors center), but without significant levels of thorium. (See Figure 5.1)

Thorium/REE particles were found in samples of Columbia river silt, waste tank farm samples, acid canyon effluent ditch, and Ganges river sediments. These particles show different anion associations depending on location found. One Thorium/REE particle found at mine along with a possible U-Pu particle at mine.

Particles studied at Hanford and Los Alamos are associated with uranium. REE particles were also found with high purity uranium oxides in Ganges river sediments, (see case 4, this chapter.)

Given the heterogeneity of the thorium distribution in the sample, particle morphology, and collocated elements, the likelihood of specific transport vectors can be more easily evaluated.

Based on the microparticle analysis, radiation in samples from this site was characterized

as containing fission products, rather than NORM. (See following page for illustration and spectra data)

Case 2 - NORM – Naturally-occurring radioactive material - Radiobismuth from Coal Ash vs. Nuclear Fuel – ***radon condensates in tobacco smoke, and lead/bismuth in coal fly ash***

Both NORM and anthropogenic radiation sources generate hot particles. Naturally occurring uranium decays into radon-222 and progeny which include radioactive forms of lead, bismuth, and polonium, Some of these same nuclides are found in anthropogenic sources such as bismuth used as a uranium carrier in nuclear reactors. These hot particles can be differentiated based on hot particle size, morphology, and trace elements.–

Radon and daughter products appear in multiple dust samples in this study. Common isotopes in this decay series include Ra 226, and daughters including Pb 210, Po 210, Bi 210. Particle sizes for condensed and nucleated radon daughters ranges from 0.02 to 0.40 microns. (George, 1991)

Coal fly ash contains uranium, thorium, and radon, based upon equilibrium with progeny. The coal fly ash also contains radioactive potassium 40. Total uranium decay series and potassium 40 content in coal ash is on the order of 300 +/- 100 Bq/Kg. (Mahur 2008)

Spent uranium nuclear fuel also contains irradiated bismuth, as uranium/bismuth alloy. Fission product particulates form from solids, rather than from nucleated gas condensates, and would be expected to produce particles above the nanometer size range.

Bismuth is a short-lived progeny of radon 226 decay, part of the uranium decay series. Bismuth is also employed as a carrier for uranium in nuclear fuel. Bismuth derived from radon decay is nanometer sized, while bismuth from nuclear processes was detected at sizes in the 2 to 20 micron range. Radiobismuth was also found in coal fly ashes, as a result of naturally occurring radioactive material.

TABLE 5.2: Below: U238 decay series showing bismuth and lead, (ref. ANL 2005)

Transition	Half-life
U-238 to Th-234	4.5 billion years
Th-234 to Pa-234	24 days
Pa-234 to U-234	1.2 minutes
U-234 to Th-230	240,000 years
Th-230 to Ra-226	77,000 years
Ra-226 to Ra-222	1600 years
Ra-222 to Po-218	3.8 days
Po-218 to Pb-214	3.1 minutes
Pb-214 to Bi-214	27 minutes
Bi-214 to Po-214	20 minutes
Po-214 to Pb-210	< 1 sec.
Pb-210 to Bi-210	22 years
Bi-210 to Po-210	5 days
Po-210 to Pb-206	140 days
Pb-206	stable

Bismuth is used as a carrier for uranium in nuclear reactor fuel. Bismuth is a short half-life daughter product of radon decay, a jacketing compound for naval reactors, and used, as bismuth phosphate, in the separation of plutonium from uranium fuels. Oil and gas industries release large amounts of radon and progeny, including bismuth isotopes. (Mudd, 2008) For a more complete description of how microanalysis distinguishes radon gas progeny bismuth from bismuth of particulate origin, see Chapter 5, Environmental significance of results.

Bismuth condensed from radon in naturally-occurring radioactive material and bismuth from fission product wastes occur as distinct hot particles, which can be isolated, analyzed, and differentiated. Specifically, bismuth condensation products are in a

nanometer size range, while anthropogenic particulate bismuth from nuclear operations is in the micron size range.

The size of radiobismuth particles can provide insight into the origin of radionuclides in environmental samples. Coal fly ash, uranium mines dusts, and natural gas soots all contain radon progeny as nanometer sized bismuth and lead particles. Bismuth is also associated with uranium fuel for nuclear reactors. Radioactive particulates from nuclear detonations and pyrolytic processes, such as the Chernobyl incident, cluster about the 0.25 to 1.0 micron size range. (Kauppinen, 1986) Dusts from fission wastes contains bismuth particles which are above 1 micron in size, and are found as large as 20 microns in select samples from this study.

Samples were analyzed for total gamma counts per second per gram using an Ortech sodium iodide detector with a Canberra shield. A series of coal fly ash samples were prepared for SEM/EDS analyses. Given the fine particle size of fly ashes, no sieving was performed on these samples.

Method: Calculate percent removal of radon progeny through Bi, Pb removal. New bismuth will be formed by decay even after initial bismuth removal, so this must be calculated. Isolation of Bismuth 214 and Bismuth 210 would create a concentrated Polonium 210 equilibrium product.

Given the short-lived nature of unstable bismuth, reanalysis of SEM targets after two to four weeks should result in significant alteration and loss of bismuth particles, and the formation of stable lead forms and polonium 210.

Stable and unstable lead is a also result of the decay of short-lived bismuth isotopes. Bismuth is associated with nuclear fuel as a carrier for uranium

Two samples of coal fly ash were acquired from Microvision Laboratories of Chelmsford, MA. The fly ash came from power generating stations in Portsmouth, NH and Salem, NH. Both fly ashes had modest levels of detectable gamma emissions, at about 2.5 and 6 CPS/g ash. Both samples displayed barely-detectable peaks, at keV levels associated with bismuth, thorium, and lead, that were just above 2X the background noise levels.

Following page: SEM photomicrographs and EDS spectra for a bismuth microparticle and a lead/bismuth microparticle seen in a coal fly ash sample.

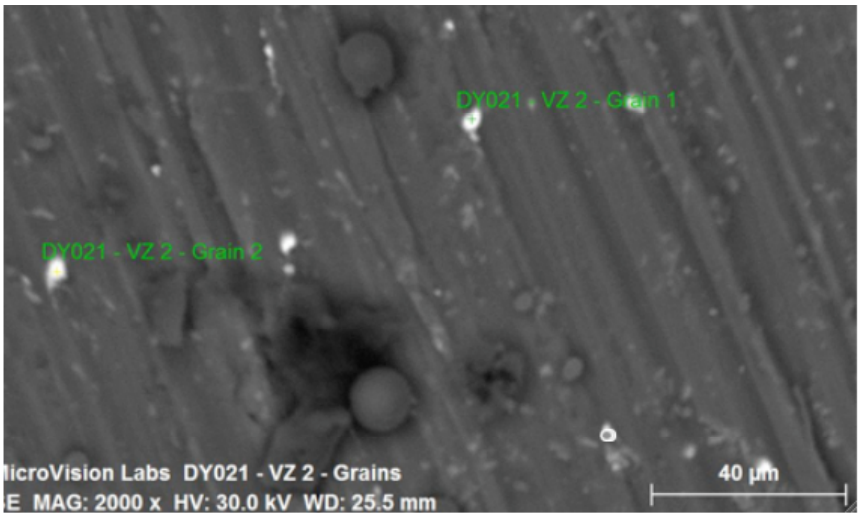
DY021 - VZ 2 - Grain 1
DY021 - VZ 2 - Grain 2
icroVision Labs DY021 - VZ 2 - Grains
E MAG: 2000 x HV: 30.0 kV WD: 25.5 mm
40 µm

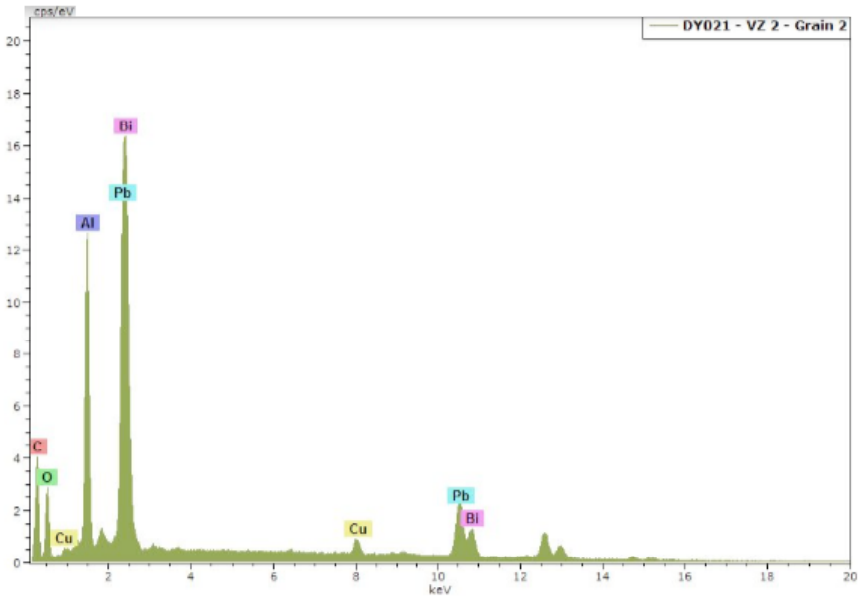
cps/eV
DY021 - VZ 2 - Grain 2
Bi
Pb
Al
C
O
Cu
Cu
Pb
Bi
keV

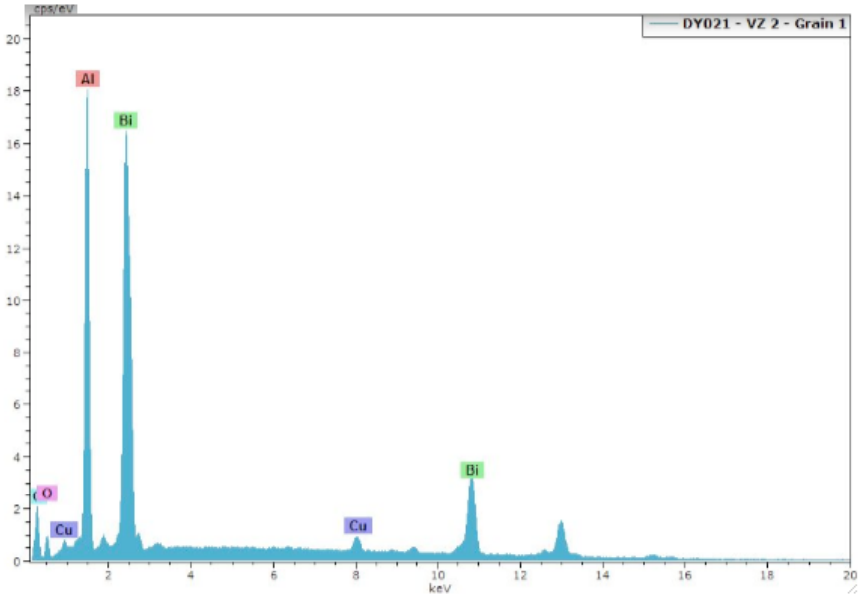
cps/eV
DY021 - VZ 2 - Grain 1
Al
Bi
O
Cu
Cu
Bi
keV

Case 3 - Midnite Uranium Mine

Dust samples were collected from structures surrounding the former Midnite Uranium Mine in Wellpinit, WA, on lands controlled by the Spokane Indian Nation. These dust samples were among the most radioactive of the environmental samples collected. After processing, SEM/EDS analysis found both uranium and thorium rare earth particles in the dusts. This site has natural geological deposits of both uranium minerals and cerium monazites.

Trace levels of radioactive isotopes were commonly detected in the set of dust samples. The radioactive isotopes found were consistent with material related to multiple sources, including radon, NORM, fallout, potassium 40, and process-related material.

Naturally-occurring radioactive material, (NORM), includes uranium and thorium isotopes naturally found in minerals. Of these isotopes, more abundant U 238 forms the basis of the radon decay series. Radon decay begins with U 238, decaying successively via Th 234 and Th 230, Ra 226, to Ra 222. Radon 222 continues to decay via lead, polonium, and bismuth isotopes into stable Pb 206.

REE are known to be associated with nuclear fission products, such as those expected at Hanford/Los Alamos, or from detonation fallout. However, it should be noted that similar spectra are associated with Cerium-monazite minerals,

Rare and isolated associations of these elements from natural fission exist at a single underground site found in Gabon, in Africa.

Ce-141, Ce-144, Nb-95, La-140, Pr-143, Pr-144 are among the principal radionuclide of reactor fission products. (Eisenbud 1963) Ce-144 in particular is the most prevalent rare earth isotope in a reactor core after 180 days of operation. (Ibid)

Kerala, India is one area known to have high levels of rare earth/thorium-bearing monazite sands in surface soils. (op cit) India supplies 71 % of worldwide monazite resources. (Government of India, Dept. of Atomic Energy, Atomic Minerals Directorate for Exploration and Research, url: http://www.dae.gov.in/amd/publicat/earv13.htm)

Xenotime particles, a Yttrium-containing mineral, were found in Ganges River sediments. Yttrium particles were also found in Los Alamos National laboratory trailer dusts. Yttrium is a component of monazite minerals. Y-90, Y-91 and Sr-90 are also among the principal radionuclides from reactor fission products. (Eisenbud 1963)

Zirconium spheres were found at Los Alamos effluent ditch and in Ganges River sediments. Zr-95 is among the principal radionuclide of reactor fission products. (Eisenbud 1963) The analysis did not provide sufficient information regarding zirconium to use its presence or absence as a basis for any environmental conclusions.

Case 4 – Ganges River Sediment

A small sample, (250 grams), of unsorted sediment was received from a climbing expedition in the Himalayas Mountains. The sample was collected from upper Ganges River sediment. The purpose of the expedition was to determine whether a thermal Pu238 power source had been lost, and possibly damaged in this area. Gross analysis of this sediment revealed traces of Pu239/240 contamination, but at a confidence level just outside of the 95 percent confidence level, and thus below the minimum quantifiable concentration. This analysis was done commercially by PACE Analytical of Pennsylvania.

No Pu238 was detected by gross analysis at PACE nor using the gamma spectrometers at WPI. The sample did not provide any data or evidence consistent with contamination from a thermal Pu238-fueled device.

Gamma spectrometry at WPI's Dept. of Physics revealed the presence of detectable quantities of U238 and U234, with total gamma activity at about 2.5 times that for uncontaminated sediments of similar composition.

This sediment sample yielded an unusually wide range of hot particles, of which 22 hot particles were analyzed individually by SEM/EDS. These 22 were a subset of the hot particles found on a single 5 cm squared monolayer of sieved sediment. Given capacity constraints, a larger number of hot particles went unanalyzed on this sample post.

The 22 hot particles detected were a mix of cerium monazites and uranium oxide particles. Interestingly, one particle consisted of high-purity uranium, with a composition of 58.0 Percent uranium, 29.1 percent oxygen, 0.34 percent lead, and 0.53 percent bismuth. The particle was approximately 20 by 25 microns in size. Its shape was crystalline subangular blocky. This is a fairly high density particle, and would be transported less effectively by flowing water than by air than would a typical, relatively lighter, soil particle. This high-purity uranium is not necessarily related to highly

enriched uranium, as no U235 specific test was performed on the hot particles.

The remaining particles were divided between lead/bismuth, or pure lead or bismuth particles, xenotime, and cerium monazite particles. The cerium monazite particles contained characteristic quantities of P, Ca, Th, and rare earth elements. Xenotime minerals contain yttrium and ytterbium.

No individual particles containing detectable amounts of any plutonium isotope were reliably detected. Based on the analysis of the hot particles in this sediment sample, it is very unlikely that the sediment contains any remnant of a plutonium 238 release. The presence of xenotime and monazites are well documented in this watershed.

Chapter 5. Conclusions

Use of sample screening, particle size fractionation, and microanalysis techniques gave good resolution of hot particle properties. This allowed for source identification in environmental samples with very low activity levels.

Chapter 6 - Future Research Goals

Future efforts will include development of a mathematical relationship describing the nature of heterogeneous radiation in dust and soil particles. This mathematical relationship should accompany the development of a quantitative procedure for determining the percentage of heterogeneous radiation compared to total uniform radiation in a population of particles. A mathematical relationship describing heterogeneous radiation should quantify the counting and detection efficiency of heterogeneous radiation in a sample, analogous to finding a means of determining the percent recovery of hot particles in a sample.

The surveillance aspect is a second area of continued experimentation, comparing civilian vs. military grade nuclear fuel production. This experiment compares samples from Hanford, WA and a civilian power fuel processor to be determined. These are generally being done on samples with very low levels of radiation.

Engineering judgments play a role in selecting dusts for sampling. Fundamental particle transport properties such as density, aerodynamic diameter, and solubility, as well as environmental behaviors such as sedimentation, erosion, and aggregate formation, need to be considered in forming an environmental sampling plan for a specific variety of hot particle. Radioactive decay and transformation impart additional variables to transport descriptions for particles, such as in the creation of solid nanoparticles of radon-progeny from radon gas.

Adding these variables to models of discrete particle transport would allow backward particle tracking of hot particles from nuclear point sources. Combined with the ability to isolate and analyze single discrete hot particles in a sample nominally at "background" levels of activity, such a model would enhance nuclear surveillance capabilities.

Future sampling and analytical efforts should include the mass spectral analyses of uranium or plutonium-bearing particulates identified by SEM/EDS. If individual uranium-bearing particles were identified, the ratio of U-235 to U-238 would identify whether the particle was of natural origin, generated from the nuclear power-generating cycle, or from weaponization programs. Extracting a uranium-positive SEM/EDS sample stub with an organic ligand, such as APDC, would yield a sample extract suitable for GC/MS analysis, and provide an isotopic breakdown. This breakdown would detail the type of nuclear program which produced the RPM, if data on size distribution, mineralization, and transport phenomena were known.

Some samples were collected but not analyzed by autoradiography or SEM/EDS based on time and funding constraints. Among these are an air filter sample, (HR0122DZ), collected from the Hanford Nuclear Reservation which displayed gamma lines for plutonium, (36.4 keV), an item from the Chernobyl reactor with Am-241 gamma lines which is thus likely to have the parent nuclide, Pu-241, engine air filter dusts which are likely to contain U-238 as depleted uranium, and sample LA0118S, a LANL-related dust sample from an area known to have some limited plutonium contamination.

Some sampling events could not be completed in time to be reviewed for this study. These include a high volume air sampler and HEPA dust filter cartridge, to be set up in Downtown Los Alamos, NM. This would allow a calculation to be made of the number of detected hot particles per unit volume of air sampled. LANL operates AIRNET, a program which produces similar air filters for gross analyses, but acquiring split samples of these filters has proven difficult. Dust samples shipped from Semipalitinsk in Kazahkstan, site of the former USSR nuclear weapons test facility, did not arrive, (and have not yet arrived), in time to be included in this study.

Chapter 7 – Conclusions

Microanalysis allows samples to be analyzed in sufficient detail to yield information about the source of discrete radionuclide particles.

The origin of radionuclide contamination in environmental samples was determined by microanalyses of individual hot particles. For individual hot particles, SEM/EDS provided sufficient data to discriminate between thorium and uranium from monazites versus fission wastes. The size, (>100 um or <100 um), sample location (in sorted silt or clothing dusts), and shape, (ultrafine aggregate or eroded) of hot particles provided evidence of airborne or waterborne transport of radionuclides, as well as natural vs. anthropogenic origins.

When required to discriminate among particles of the same radioisotope, such as with bismuth from fission waste vs. bismuth from radon exhalation. Bismuth from fission wastes were visible in dust collected from radiological operations at Los Alamos National Laboratory. (This sample, LA0100D, was collected from vacuum cleaner bag dust taken from a trailer at the time is was transported from the National Laboratory, in preparation for the trailer to be sold as surplus property.) Bismuth, presumed to be from radon exhalation, was detected by Robinson/SEM/EDS in coal fly ashes, at diameters between 1 and 10 microns. This is larger than typical, and likely represents the formation of aggregates of finer matter. In both cases, bismuth was found neat, and as mixtures with lead. Lead and bismuth are both in the radon decay chain.

Once hot particles had been isolated from a sample, useful environmental radiological information was gained from samples whose gross radioactivities were close to background levels.

Individual hot particles were detected from these samples, having multiple sources of radionuclides, could be distinguished, even when the nuclide(s) of interest was(were) identical.

Microanalysis was more sensitive than the gross analyses of bulk samples. Microanalysis was less subject to signal noise created by dilution of contaminants in the environment. Biased sampling of environmental media allowed the collection of hot particles, which were further concentrated from bulk samples via size fractionation. Autoradiography was used to confirm the presence, and map the location, of hot particles for further analysis by SEM/EDS. All 114 samples of dust, sediments, and other materials, reviewed for this study were between 0.9 and 5.0 times the total activity of null count background samples. For the majority of these samples tested by SEM/EDS, the radionuclides contributing to total sample activity were ones which have multiple natural and anthropogenic sources, such as isotopes of Bi, U, Th, Ra, Ce, La, Nd, Sm, Gd, and Pb. For the remaining samples which had detectable hot particles, nuclides from multiple anthropogenic sources were also detected including isotopes of Pu, Np, Am, Sr, and Cs. Samples of river sediments with thorium from monazites, clothing dusts with thorium from monazites, and fission wastes with thorium from spent fuel, were all distinguished.

The origin of radionuclide contamination in environmental samples was elucidated by microanalyses of individual hot particles.

Examples include the finding of supra-micron sized bismuth particles in Los Alamos NL dust samples., such as the discovery of cerium monazites as the source of thorium activity in Columbia River sediment. Hot particles allowed thorium rare earth particles related to monazite deposits to be distinguished from thorium rare earth particles related to nuclear fission wastes, as in the monazites from India, Spokane, and the Columbia River at Richland, vs. thorium rare earth deposits at the Los Alamos NL former WWTP effluent ditch.

Hot particles accounted for a significant fraction of total gross radioactivity in environmental samples.

Simple mathematical treatment of the SEM/EDS and other data allows for a determination of the percentage of radioactivity in an environmental sample which can be demonstrated to be heterogeneous. This calculation requires knowing the total measured activity, counting efficiency, size and geometry of hot particles, radionuclide identity and density, as well as developing a relatively efficient hot particle separation scheme.

Radioactive heterogeneity in a sample of particulate matter can be quantified with a simple set of mathematical expressions.

The activity in a sample or population of particles can be described by the following mathematical expression. This expression is practical and measurable, incorporating an approximation of particle volume, based on particle area. Areas can be determined practically by SEM. Given the limited numbers of high activity particles found in the environmental samples tested in this study, this equation is solvable using very limited caculation times. For samples at environmentally important levels, (for example, 5 pCi/g, the CERCLA total alpha emission limit for soils), the calculation can require review of very few particles. For radium 226 activity, for instance, as few as two 1.0 micron diameter radium 226 particles can prodiuce all the activity in and otherwise inert gram of sample.

$$\text{Activity} = 4\pi/3 \sum (\text{area}_j^{3/2} \times \sum (\text{SA}_i \times \text{MF}_i \times \text{density}_i))$$

A more computationally intensive version of this expression would employ a rotation of the actual two dimensional shape, (as determined by SEM), to yield a volume, rather than assuming sphericity. The method remains a practical rather than an exact expression, but adds an electronic computation to find the volume, yielding a more precise result.

$$\text{Activity} = \sum \left(f(\text{area}_j) \times \sum \left(SA_i \times MF_i \times \text{density}_i \right) \right)$$

Solutions to these equations are practical for heterogeneous samples, meaning that the calculations are straightforward, finite, and with a unique solution, given sufficient data. Homogenous samples are described by the expression.

$$\text{Activity} = \text{Sample Mass} \times \sum \left(SA_i \times MF_i \right)$$

The radioactive heterogeneity of a sample is described by the expression below.

$$\text{Heterogeneity} = - \text{Log} \ (1.67 \times n / N)$$

For relatively heterogeneous samples collected for this study, n / N was approximately 1 / 5000. (Based on autoradiography to determine n, the number of radiation carrying particles, and optical miscopy to estimate N, the total number of particles in the sample). The sample heterogeneity for this example is 3.5.

As n approaches N, the value of this function rapidly decreases. Small values of n / N, indicate increasing radioactive heterogeneity, and the function increases in magnitude. This function decreases below 0.001 as n approaches 0.6 times N, meaning as the sample is more uniform in its distribution of specific activity. The value of n/N must be nonzero and positive.

8 - References

Sajo-Bohus, L., (1998), Hot Particle Spectrum Determination by Track Image Analysis, Radiat. Phys. Chem., V 51, No 4-6, pp 467-468

Lang, S., Servomaa, K., Kosma, V.-M., Rytomaa, T., (1995), *Biokinetics of Nuclear Fuel Compounds and Biological Effects of Nonuniform Radiation*, Environmental Health Perspectives, Vol. 103, No. 10. Oct., pp. 920-934.

Broda, R., (1987), *Gamma Spectroscopy Analysis of Hot Particles from the Chernobyl Fallout,* Acta Physica Polonica, B18 (10), pp. 935 – 950

Eisenbud, M., and Harley, J., (1953), *Radioactive Dust from Nuclear Detonations*, Science, New Series, Vol. 117, No. 3033, Feb. 13, pp. 141-147

Eisenbud, M., (1963), Environmental Radioactivity, McGraw-Hill

Clark, H. M., (1954), *The Occurrence of an Unusually High-level Radioactive Rainout in the Area of Troy, NY*, Science, 119:619

Akhtar, N., et al, (2005), *Natural environmental radioactivity and estimation of radiation exposure from saline soil*, International Journal of Environmental Science & Technology, Vol. 1, No. 4, pp. 279-285,

Cizdziel, J. V., (a) Hodge, V. F.,(b) (2000), Attics as archives for house infiltrating pollutants: trace elements and pesticides in attic dust and soil from southern Nevada and Utah, Microchemical Journal 64 2000 85 92, (a) Environmental Science and Health Program, University of Nevada Reno, Reno, NV 89557-0187, USA, (b) Department of Chemistry, University of Nevada Las Vegas, 4505 Maryland Pkwy, Las Vegas, NV 89154-4003

Argonne National Laboratory, (2005), *Natural Decay Series: Uranium, Radium, and Thorium*, EVS Human Health Fact Sheet, August

Lewis, Robert G., (1999), *Distribution of Pesticides and Polycyclic Aromatic Hydrocarbons in House Dust as a Function of Particle Size*, Environmental Health Perspectives V 107, No. 9, Sept.

Radford, Edward P., (1985), *Potential Health Effects of Indoor Radon Exposure*, Environmental Health Perspectives, V. 62, p 281-287

Lioy, (2002), *Dust: A Metric for Use in Residential and Building Exposure Assessment and Source Characterization*, Environmental Health Perspectives, V 10, No. 10, 969 - 983

Lioy, (2003), *The historical record of air pollution as defined by attic dust, Atmospheric Environment*, 37, 2379 – 2389

Patton, et al, (2005), Pacific Northwest National Laboratory, *Survey of Potential Hanford Site Contaminants in the Upper Sediment for the Reservoirs at McNary, John Day, The Dalles, and Bonneville Dams, 2003*

Hamilton, E. I., (1966), *Distribution of Uranium in Some Natural Minerals*, Science, New Series, V 151, No. 3710, Feb. 4, 1966, pp. 570-572

Shleien, B., et al, (1965), *Particle Size Fraction of Airborne Gamma-Emitting Radionuclides by Graded Filters*, Science Vol. 147 p. 290

Friedlander, S.K., (2000), *Smoke, Dust, and Haze, Fundamentals of Aerosol Dynamics*, 2nd Ed., Oxford University Press

Knoll, G. F., (2000), *Radiation Detection and Measurement*, 3rd Ed., John Wiley and Sons, Inc.

Agency for Toxic Substances and Disease Registry, ATSDR, U.S. Public Health Service, (2004), TOXICOLOGICAL PROFILE FOR AMERICIUM, DEPARTMENT OF HEALTH AND HUMAN SERVICES

Agency for Toxic Substances and Disease Registry, ATSDR, U.S. Public Health Service, (2004), TOXICOLOGICAL PROFILE FOR CESIUM, DEPARTMENT OF HEALTH AND HUMAN SERVICES

Agency for Toxic Substances and Disease Registry, ATSDR, U.S. Public Health Service, (2007), TOXICOLOGICAL PROFILE FOR PLUTONIUM, DEPARTMENT OF HEALTH AND HUMAN SERVICES

Agency for Toxic Substances and Disease Registry, ATSDR, U.S. Public Health Service, (2002), *Case Studies in Environmental Medicine, Radiation Exposure from Iodine 131*, DEPARTMENT OF HEALTH AND HUMAN SERVICES

Agency for Toxic Substances and Disease Registry, ATSDR, U.S. Public Health Service, (2007), RADIOACTIVE CONTAMINATION FROM THE MIDNITE MINE SITE, WELLPINIT, STEVENS COUNTY, WASHINGTON, EPA FACILITY ID: WAD980978753, APRIL 10, 2007

Sposito, G., (1989), *The Chemistry of Soils*, Oxford University Press, New York, NY

Sposito, G., (2008), *The Chemistry of Soils*, *2nd Ed.* Oxford University Press, New York, NY

U.S. Dept. of Energy, (2003), *Hanford Site Historic District: History of the Plutonium Production Facilities, 1943 – 1990*, Hanford Cultural and Historic Resources Program, Rodriguez, A.L., Lloyd, D., Director; Batelle Memorial Institute, Columbus, OH

Argonne National Laboratory, (2005), Potassium 40 Human Health Factsheet, August

US Environmental Protection Agency, (2005), *EMERGENCY RESPONSE QUALITY ASSURANCE SAMPLING PLAN, HURRICANE KATRINA RESPONSE, Screening Level Sampling for Sediment in Areas Where Flood Water Receded SOUTHEAST, LOUISIANA*, September, pp. 8 - 9

Strezov, A., (1996), *Natural Radionuclides and Plutonium Content in Black Sea Bottom Sediments*, Health Physics Society, p. 70-79

George, A.C. et al, (1991), Abstract: *Indoor radon progeny aerosol size measurements in urban, suburban, and rural regions*, Aerosol Science and Technology, v 15, n 3, Oct, p 170-178

McNaughton, (2008), Los Alamos National Laboratory publication LA-UR 08-07159, Dec. 10.

Stover, B. J., (1972), Radiobiology of Plutonium, as cited in Los Alamos Science, No. 23, 1995, p. 24

Utsunomiya, Satoshi, (2009), Dekker Encyclopedia of Nanoscience And Nanotechnology, CRC PRESS, Ch. 110., Environmental Electron Microscopy Imaging, pp. 1 to 10.

Filippidis, Anestis, (1997), *Mineral, Chemical and Radiological Investigation of a Black Sand at Touzla Cape, near Thessaloniki, Greece*, Environmental Geochemistry and Health, 19, 83-88

F. Wagenpfeil, (1999), *Resuspension of coarse particles in the region of Chernobyl*, Atmospheric Environment 33, 3313 - 3323

Mike McNaughton, (2008), environmental surveillance manager LANL, personal communication

John Brodeur, (2008), a Washington State registered professional civil engineer, personal communication

Rudi H. Nussbaum, (2008), Portland State University, personal communication

Englert, D., et al, (2007), *Distribution of Radionuclides in Northern Rio Grande Fluvial Deposits near Los Alamos National Laboratory, New Mexico*, Department of Energy Oversight Bureau, New Mexico Environment Department

Hoyt, M, (2009), Analyses of Nanoparticles in the Environment, Chapter 5, pp. 99-122

Vlasova, I. E., (2006), *Radiography and Local Microanalysis for Detection and Examination of Actinide-Containing Microparticles*, Radiochemistry, Vol. 48, No. 6, pp. 613-619.

The Science News-Letter, (1939), *Release Atomic Energy from Massive Thorium*, Vol. 35, No. 7, (Feb. 18), pp. 102

Mahur, A.K., (2008), *Estimation of radon exhalation rate, natural radioactivity and radiation doses in fly ash samples from Durgapur thermal power plant, West Bengal, India*, Journal of Environmental Radioactivity 99, 1289–1293

McCubbin, David, (2000), *Association of 210Po, 210Pb, 239+240Pu and 241Am with different mineral fractions of a beach sand at Seascale, Cumbria, UK*, The Science of the Total Environment 254, 1-15

Kauppinen, Esko, (1986), *Radioactivity Size Distribution of Ambient Aerosols in Helsinki, Finland, during May 1986 after the Chernobyl Accident: Preliminary Report*,

Environ. Sci. and tech., V 20, No. 12, pp 1257 - 1259

Kovler, K., et al. (2005), *Radon exhalation of cementitious materials made with coal fly ash: Part 1 - scientific background and testing of the cement and fly ash emanation,* J. Environ. Radioactivity 82, 321 - 334

Trabalka, J., (1980), *Analysis of the 1957-1958 Soviet Nuclear Accident*, Science Pub.: 1980-07-18, Volume: 209, Issue: 4454, Pages: 345-353

Mudd, G., (2008), *Radon sources and impacts: a review of mining and non-mining issues,* Springer Science Business Media B.V. 2008, Rev. Environ Sci Biotechnol, 7:325–353, DOI 10.1007/s11157-008-9141-z

Pacific Northwest National Laboratory, PNNL, (2005), Environmental Surveillance document, U.S. Dept. of Energy

Kaltofen, M.P.J. and Carpenter, T., (2005), *Citizens Environmental Monitoring at the Hanford Reach of the Columbia River*, report published by the Government Accountability Project, Oct.

Michel R, Klipsch K, et al., (2005), *Long-lived Radionuclides in the Environment: On the Radioecology of Iodine-129,* Radioprotection, 40 (Suppl.1): S269 1596

Ersahin, S., (2006) *Estimating specific surface area and cation exchange capacity in soils using fractal dimension of particle-size distribution*, Geoderma, V 136, Issues 3-4, 15 December, 588-597

Parrish, R. R., (2008), *Depleted uranium contamination by inhalation exposure and its detection after 20 years: Implications for human health assessment*, Science of the Total Environment, 390, pp. 58 – 68

Hochella, M.F. Jr., (1990), Mineral-Water Interface Geochemistry, Reviews in Mineralogy (23), Mineralogical Society of America

Yalcin, S., (2007), *Calculation of total counting efficiency of a NaI(Tl) detector by hybrid Monte-Carlo method for point and disk sources, Applied Radiation and Isotopes*, V 65, pp. 1179 – 1186.

U.S. Dept. of Energy, (2004), Office of Legacy Management, Acid/Pueblo Canyon, New Mexico Site Factsheet

Los Alamos National Laboratory, (2007), *Environmental Surveillance at Los Alamos During 2007*, Executive Summary, LA-14369-ENV, National Nuclear Security Administration

Isosaari, P., (2001), *Use of Olive Oil for Soil Extraction and Ultraviolet Degradation of Polychlorinated Dibenzo-p-dioxins and Dibenzofurans*, Environmental Science and Technology, 35, 1259-1265.

Terry E.C, (1983), *Selective concentration of cesium in analcime during hydrothermal alteration, Yellowstone National Park, Wyoming*, Geochimica et Cosmochimica Acta V. 47, No. 4 , 795 - 804

Sturchio, N.C., (1987), *Thorium - uranium disequilibrium in a geothermal discharge zone at Yellowstone,* Geochimica et Cosmochimica Acta V. 51, No. 7, Pages 2025 - 2034